



Programme: VLT

Project/WP: MUSE

MUSE User Manual

Document Number: ESO-261650

Document Version: 7.3

Document Type: Manual (MAN)

Released On:

Document Classification: Public

Prepared by: J. Richard, R. Bacon and J. Vernet

Validated by: C. Dumas

Approved by: A. Kaufer

Maintained and Edited by: F. Selman and E. Johnston



Authors

Name	Affiliation
J.Richard and R. Bacon	Original authors from MUSE Consortia
E. Johnston & F. Selman	Editor and maintainer DOO

Change Record from previous Version

Affected Sections(s)	Affected Section(s)	Changes / Reason / Remarks
all	2017-01-13	All cross-references to figures and tables corrected and fixed (EJo)
5.1	2017-06-14	Update to include information about p2 and the unified GuideCam tool (EJo)
8.0	2017-06-29	Added information on GALACSI and GLAO observations. All sections affected.



Contents

1	Introduction	7
1.1	Scope.....	7
1.2	The MUSE Facility in a nutshell.....	7
1.3	More information on MUSE Facility	9
1.4	Version notes, change track	9
	• Version 8	9
	• Version 7	9
	• Version 6	9
	• Version 5.10	10
	• Version 1.3.1	10
	• Version 1.3.0	10
	• Version 1.1	10
	• Version 1.0	10
1.5	List of Abbreviations & Acronyms	10
2	Technical description of the MUSE Facility	13
2.1	Technical Description of MUSE	13
1.1.1	Overview of the opto-mechanical design.....	13
1.1.2	Description of the instrument sub-systems.....	14
1.1.2.1	Calibration Unit.....	14
1.1.2.2	Fore Optics.....	16
	• Derotator	16
	• Filter Wheel	16
	• Mode-switching unit and Atmospheric Dispersion Corrector (NFM only).....	16
	• IRLOS (NFM only).....	16
	• Anamorphoser.....	16
	• Slow Guiding System (SGS)	17
	• Exposure shutter	17
1.1.2.3	Splitting and Relay Optics (SRO) system	18
1.1.2.4	Integral Field Unit	20
1.1.2.4.1	Slicer.....	21
1.1.2.4.2	Spectrograph	21
1.1.2.4.3	Detector	21
1.1.2.5	Spectral format.....	23
1.2	Technical Description of GALACSI and the AOF	24
1.2.1	Overview of the Adaptive Optics Facility (AOF)	24



1.2.1.1	The Deformable Secondary Mirror (DSM)	24
1.2.1.2	The Four Laser Guide Star Facility (4LGSF)	26
1.2.2	Overview of GALACSI	26
1.2.2.1	Wide Field Mode	26
1.2.2.2	Narrow Field Mode	28
3	Overall performances and characteristics	28
3.1	Absolute throughput and limiting magnitude	28
3.2	Spectral resolution and sampling	29
3.3	Exposure timing	30
3.4	Overall illumination and uniformity	30
3.5	Distortion and astrometric precision	31
3.6	Second order contamination	31
3.7	Image Quality Gain in WFM AO	32
3.8	Instrument stability	33
4	Problems to be aware of	35
4.1.1	Ghosts, straylight, spikes and ferris wheels	35
4.1.2	Remanence	35
4.1.3	Detector defects	35
4.1.4	Bad columns/pixels	36
4.1.5	Contamination caused by Na Laser during AO observations	36
4.1.6	Regions of reduced sensitivity on flat fields	36
5	Observing with MUSE	38
5.1	General information	38
5.2	MUSE Observing modes	38
5.3	MUSE Target acquisition	39
5.4	MUSE science observations	42
5.5	Attached calibrations	46
5.6	Instrument and Telescope Overheads	46
6	Calibrating and Reducing MUSE data	48
6.1	MUSE calibration plan	48
6.1.1	Wavelength calibration	49
6.1.2	Flat-field calibration	49
6.1.3	Nightly illumination correction	49
6.1.4	Twilight sky flat calibration	49
6.1.5	Geometrical (spatial) calibration	49
6.1.6	Spectro-photometric calibration	50
6.1.7	Telluric Correction	50



6.2	MUSE data reduction.....	51
7	Templates	53
7.1	MUSE acquisition templates.....	53
7.1.1	MUSE_wfm-noao_acq_movetopixel template signature file	53
7.1.2	MUSE_wfm-ao_acq_movetopixelLGS template signature file	53
7.1.3	MUSE_wfm-noao_acq_preset template signature file	54
7.1.4	MUSE_wfm-noao_acq_presetRRM template signature file	54
7.2	Observation Templates Tables.....	56
7.2.1	MUSE_wfm-noao_obs_genericoffset template signature file.....	56
7.2.2	MUSE_wfm-ao_obs_genericoffsetLGS template signature file.....	57
7.3	Calibration Templates Tables	57
7.3.1	Templates specifically written for night astronomers.....	57
7.3.1.1	MUSE_wfm_cal_waveatt	57
7.3.1.2	MUSE_wfm_cal_specflatatt	58
7.3.2	Other calibration templates.....	59
7.3.2.1	MUSE_cal_bias template signature file	59
7.3.2.2	MUSE_cal_dark template signature file	59
7.3.2.3	MUSE_wfm_cal_geometry template signature file	59
7.3.2.4	MUSE_wfm_cal_specflat template signature file	60
7.3.2.5	MUSE_wfm_cal_wave template signature file	60
7.3.2.6	MUSE_wfm_cal_twilight template signature file	61
7.3.2.7	MUSE_wfm_cal_specphot template signature file.....	61
7.3.2.8	MUSE_wfm_cal_telluric template signature file	62
7.3.2.9	MUSE_wfm_cal_astrom template signature file	62
8	Reference material	64
8.1	Detector cosmetics	64
8.2	Arc lamps list.....	65
8.2.1	HgCd arc lamp.....	65
8.2.2	Xe arc lamp	66
8.2.3	Ne arc lamp	68
8.3	Description of the WFM_SMP mask.....	70
8.4	Log of instrument changes	71
8.5	ds9 template	71



MUSE User Manual

Doc. Number: ESO-261650

Doc. Version: 7.00

Released on:

Page: 6 of 72

1 Introduction

1.1 Scope

The MUSE User Manual was written and provided to ESO by John Richard and Roland Bacon from the MUSE consortium. It is maintained by the ESO Paranal Instrument Scientist and the MUSE Instrument Operation Team (IOT). It provides extensive information on the technical characteristics of the instrument, its performances, observing and calibration procedures and data reduction. The goal is to provide all pieces of information and advice necessary for MUSE users to prepare their observations. It is intended for MUSE users, and as such it is written from an astronomer's perspective.

We welcome any comments and suggestions on this manual; these should be addressed to the User Support Group at usd-help@eso.org.

1.2 The MUSE Facility in a nutshell

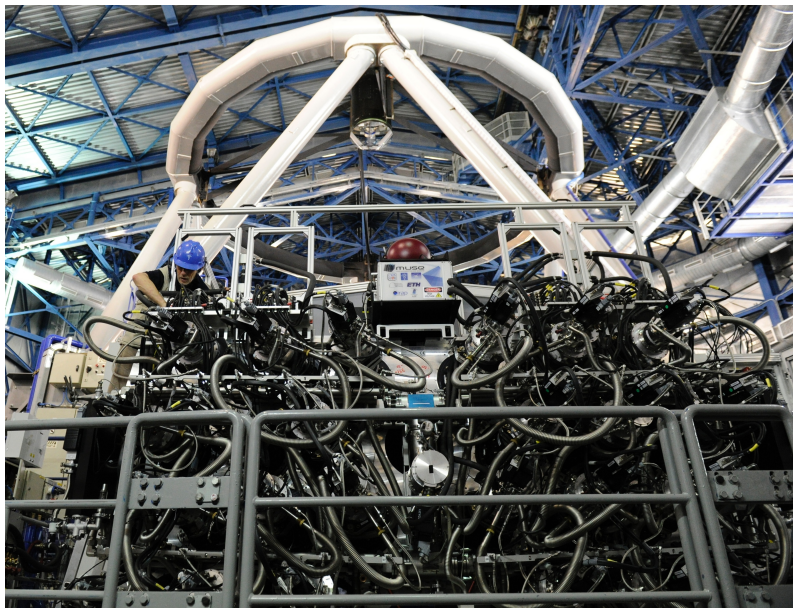


Figure 1: MUSE at the Nasmyth B focus of Yepun (UT4).

MUSE, the **M**ulti **U**nit **S**pectroscopic **E**xplorer, is a second-generation VLT instrument located on the Nasmyth platform B of the VLT UT4. It is a large-format integral-field spectrograph, based on image-slicing technology, and has a modular structure composed of 24 identical Integral Field Unit modules that together sample a contiguous 1 arcmin² field of view in Wide Field Mode (WFM) sampled at 0.2 arcsec/pixel. Spectrally, the instrument samples most of the optical domain, with a mean resolution of 3000. MUSE is currently used in WFM only.

MUSE exploits the VLT Adaptive Optics Facility (AOF) at the VLT UT4 (Yepun) with its 4 Laser Guide Stars (4LGSF) and the Deformable Secondary Mirror (DSM) in combination with **GALACSI**, the **G**round **A**tmospheric **L**ayer **A**daptive **C**orrector for **S**pectroscopic **I**maging, which provides Ground Layer Adaptive Optics (GLAO) correction for the WFM.



In the future, a Narrow Field Mode (NFM) will also be made available, and will cover a ~ 7.5 arcsec² field of view sampled at 0.025"/pixel with Laser Tomography AO correction. The combination of MUSE and GALACSI is named **MUSE Facility**.

A view of the instrument attached to the telescope is shown in Figure 1. The main instrument characteristics are summarized in Table 1.

The MUSE instrument was built by a Consortium involving institutes from France, Germany, The Netherlands, Switzerland and ESO. The GALACSI AO module was built by ESO as part of the AOF project. The names of the institutes and their respective contributions are given in Table 2.

Table 1: MUSE in a nutshell.

Number of modules	24
Wavelength range	480 – 930 nm (nominal) 465 – 930 nm (extended)* Wavelength range excluded for AO observations (Na Notch filter): 582 – 597 nm (nominal) 578 – 599 nm (extended)
Resolving power	1770 (480 nm) – 3590 (930 nm) (WFM) 1740 (480 nm) – 3450 (930 nm) (NFM)
Spectral sampling	0.125 nm/pixel
Detectors (per module)	4k x 4k e2V CCD
Field of view	59.9" x 60.0" (WFM) 7.42" x 7.43" (NFM)
Spatial pixel scale	0.2" / pixel (WFM) 0.025" / pixel (NFM)
Throughput (total atmosphere, telescope and instrument)	14 % (480 nm) 33 % (750 nm) 14 % (930 nm)

(*) only available for WFM instrument modes. Suffers from 2nd order contamination



1.3 More information on MUSE Facility

All MUSE Manuals are available on the MUSE instrument WEB pages, together with the most updated information on the instrument:

<http://www.eso.org/sci/facilities/paranal/instruments/muse/>

Information and software tools for the preparation of service and visitor mode observations with MUSE are available at:

<http://www.eso.org/sci/observing/phase2>

<http://www.eso.org/sci/observing/phase2/SMGuidelines.html>

Work based on MUSE observations should cite the paper:

[Bacon et al., Proc of the SPIE, Vol. 7735, 7 \(2010\)](#)

Work based on observations with Adaptive Optics should also cite:

[Stroebele et al., Proc. of the SPIE, Vol. 8447, 11 \(2012\)](#) and

[Arsenault et al., Proc of the SPIE, Vol. 7736 \(2010\).](#)

Visiting astronomers will find further instructions on the Paranal Science Operations WEB page and the Paranal Observatory home page:

<http://www.eso.org/sci/facilities/paranal/>

<http://www.eso.org/sci/facilities/paranal/sciops/>

There is also a MUSE forum for questions concerning observing and data reduction strategies, you will be able to reach the forum by going to:

<http://www.eso.org/sci/data-processing/forum.html>

We recommend that any questions that you might have be addressed in the FORUM. This way others may benefit from the answers.

1.4 Version notes, change track

- Version 8
Document upgraded to include information on GALACSI and WFM AO observations
- Version 7
Uncorrupted version. All table and Figure numbers now correct.
- Version 6
Several links have been updated. This version should be used for P97 Phase II onwards.



- **Version 5.10**

In this version we changed the versioning number to the PDM scheme.

Released for P96 Phase II. Note that this version documents the recent changes to the detector system including the change of detector in channel 01 to eliminate the problem of the glowing pre-amplifier. To reduce bias and dark structure we are now continuously wiping the CCDs between exposures.

- **Version 1.3.1**

Released for P96 Phase I on 4 March 2015. Minor change added RRM acq_Preset template info.

- **Version 1.3.0**

Released for P95 Phase I on 8 Sep 2014. Note that there was no version 1.2

- **Version 1.1**

This version was released for P94 Phase II.

- **Version 1.0**

The first version of this manual has been delivered by the MUSE consortium, P.I. R. Bacon, for Phase I, P94, on 28 Feb 2014.

1.5 List of Abbreviations & Acronyms

This document employs several abbreviations and acronyms to refer concisely to an item, after it has been introduced. The following list is aimed to help the reader in recalling the extended meaning of each short expression:

4LGSF:	Four Laser Guide Stars Facility
ADC:	Atmospheric Dispersion Corrector
ADU:	Analog / Digital Unit
AO:	Adaptive Optics
AOF:	Adaptive Optics Facility
CCD:	Charged Coupled Device
CU:	Calibration Unit
DQ:	Data Quality
DRS:	Data Reduction Software
DSM:	Deformable Secondary Mirror
ESO:	European Southern Observatory
FO:	Fore Optics
FOV:	Field Of View
GALACSI	Ground Atmospheric Layer Adaptive Corrector for Spectroscopic Imaging
GLAO:	Ground Layer Adaptive Optics
HST:	Hubble Space Telescope
IFU:	Integral Field Unit
IOT	Instrument Operation Team
IRLOS:	Infrared Low Order Sensor
IS	Instrument Scientist



LGS:	Laser Guiding Star
LSF:	Line Spread Function
LTAO:	Laser Tomography Adaptive Optics
MUSE:	Multi Unit Spectroscopic Explorer
NFM:	Narrow Field Mode
NGC:	New Generation Controller
OGS:	On-axis Guide Star
p2:	Phase 2 tool (Visitor mode)
P2PP tool:	Phase 2 Proposal Preparation tool (Service mode)
QE:	Quantum Efficiency
RON:	Read Out Noise
RMS:	Root Mean Square
RTD:	Real Time Display
SGS:	Slow Guiding System
SNR:	Signal to Noise Ratio
SRO:	Splitting and Relay Optics
TBC:	To Be Confirmed
TSF:	Template Signature File
TTS:	Tip-Tilt Star
USD:	User Support Department
UT:	Unit Telescope
VLT:	Very Large Telescope
WFM:	Wide Field Mode

**Table 2:** collaborating institutes and their contributions.

Collaborating institutes	Contribution
Leibniz-Institut für Astrophysik Potsdam	Development of the Calibration Unit, testing of the preassembled spectrograph-detector units, data reduction software
Centre de Recherche Astrophysique de Lyon	Overall management of the project, image slicer sub system, spectrograph opto-mechanical design and integration, data analysis software.
ESO	Detector systems (24 detectors and their cryogenic environment, Adaptive Optics Facility (AOF) including the GALACSI Adaptive Optics module, the Laser Guide Star Facility (4LGSF) and the Deformable Secondary Mirror (DSM)
ETH – Institute of Astronomy (Zurich)	Procurement of the 24 spectrographs
Institut für Astrophysik Göttingen	Design, analysis and procurement of the instrument mechanics, the support and handling structures as well as for the optics that apply the field splitting and the relay optics.
Institut de Recherche en Astrophysique et Planétologie (Toulouse)	Electronic and Software Control of the whole Instrument, Opto-mechanical development of the Fore-Optics module.
Leiden Observatory	Interface between the MUSE spectrograph and the adaptive optics system, definition of the top-level requirements for the adaptive optics system.

2 Technical description of the MUSE Facility

2.1 Technical Description of MUSE

1.1.1 Overview of the opto-mechanical design

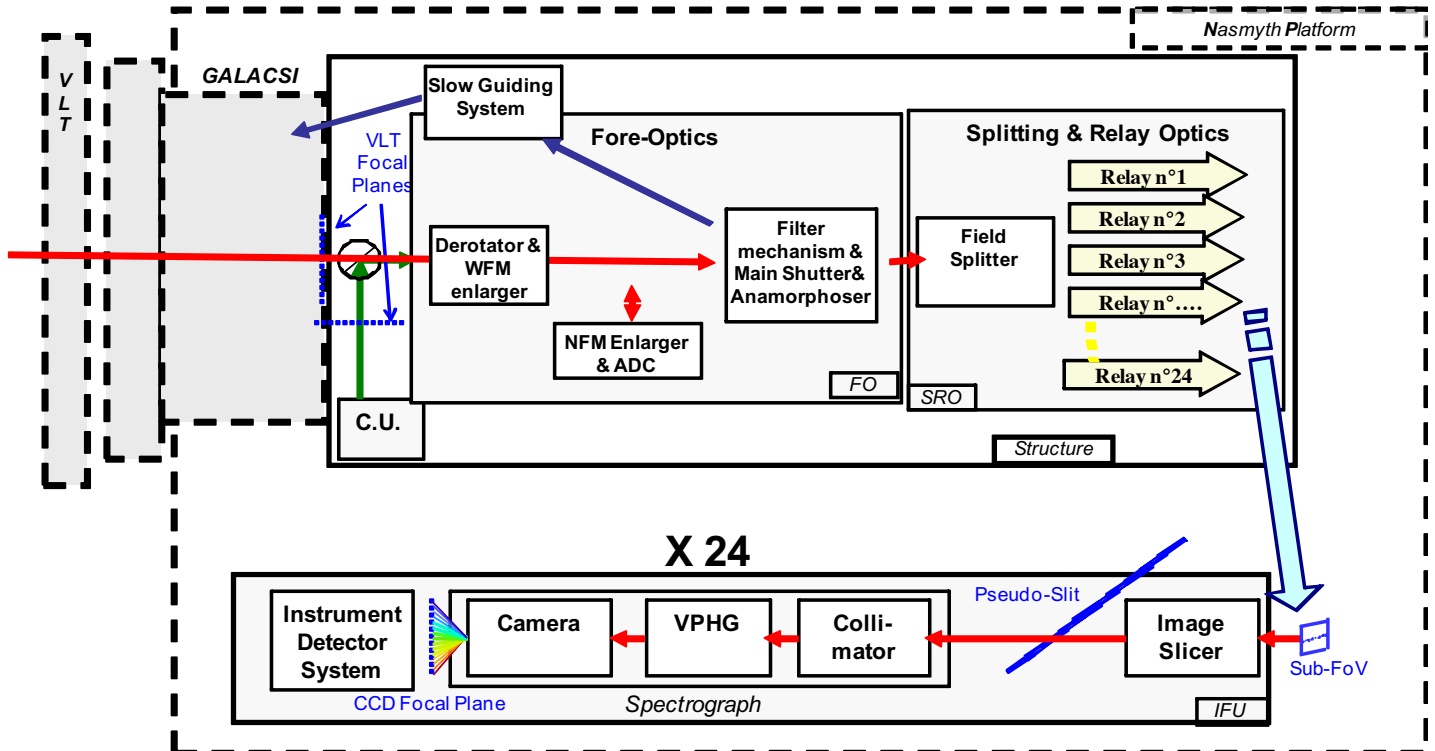


Figure 2: Overview of MUSE subsystems.

Figure 2 shows a schematic view of the layout of MUSE. The instrument is composed of the following sub-systems:

- The **Calibration Unit** (CU) provides different illumination fields to calibrate MUSE instrument. It includes functions to switch on and off the lamps, motors to position the chosen mask and to insert a Calibration pick-up mirror in the MUSE instrument light path. These functions are controlled through calibration and maintenance templates.
- The **Fore Optics** (FO) reshapes the VLT focus image to adapt it to the next sub-system, which splits the image in 24 channels. It rotates the field, magnifies it, and reshapes it into a 2:1 ratio.
- The **Splitting and Relay Optics** (SRO) sub-system divides the Field of View (FOV) in 24 horizontal sub-fields, and feeds each Integral Field Unit.
- Each of the **24 Integral Field Units** (IFU) is composed of 3 sub-systems: the Image Slicer, the Spectrograph, and the Detector. Each IFU observed one of 24 sub-fields within the field-of-view, and each image slicer further subdivides this sub-field into 48 slices.



1.1.2 Description of the instrument sub-systems

This section describes the different sub-systems of MUSE in the order they are encountered along the optical path going from the telescope to the detectors (see Figure 2 and Figure 3). The functionalities of the different sub-units are explained and reference is made to their measured performance.

1.1.2.1 Calibration Unit

The calibration unit (CU) is a mechanical structure with calibration lamps, an integrating sphere, and a set of masks used to produce calibration fields for MUSE. A calibration pick-up mirror is used to direct light into the instrument from either the telescope or the CU.

The CU allows for a choice of **6 calibration lamps** as input light sources:

- Two flat-field halogen lamps providing uniform continuum flux over the MUSE wavelength range
- 4 arc lamps used for wavelength calibration:
 - One Ne pencil-ray lamp
 - One Xe pencil-ray lamp
 - One HgCd pencil-ray lamp
 - One Ne High Power lamp

Two pico-ampere meters placed at the CU focal plane are used to monitor the absolute flux sent by the lamps into MUSE. Details on the line wavelengths and relative fluxes produced by each lamp are provided in Section 8.2

The **focal plane mask wheel** allows for a choice of 5 masks covering the CU FOV. Two positions are used in regular operation: CLEAR and WFM_SMP.

- The CLEAR (no mask) position is used for flat-field and wavelength calibrations.
- The WFM_SMP is a mask containing a grid of small (50 μ m diam.) pinholes covering the WFM FOV. It is used to perform the geometrical calibration (see Section 8.3).

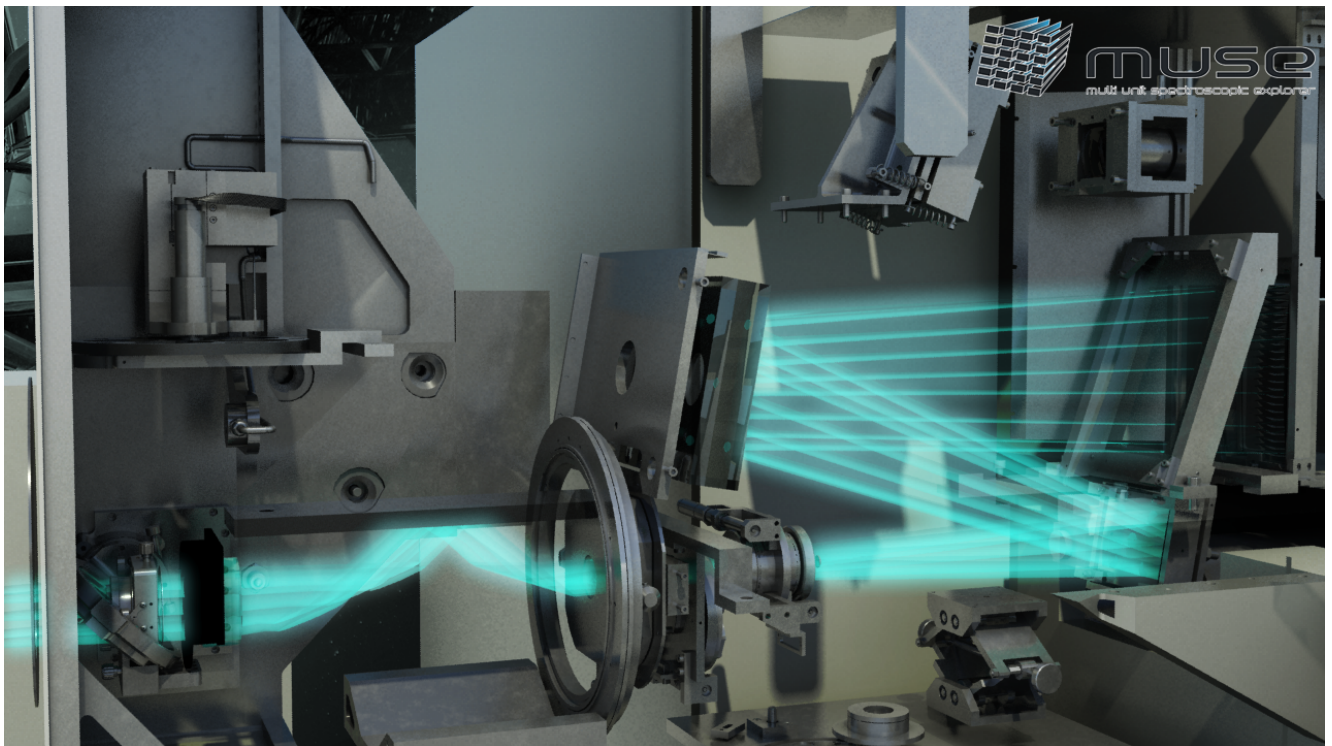
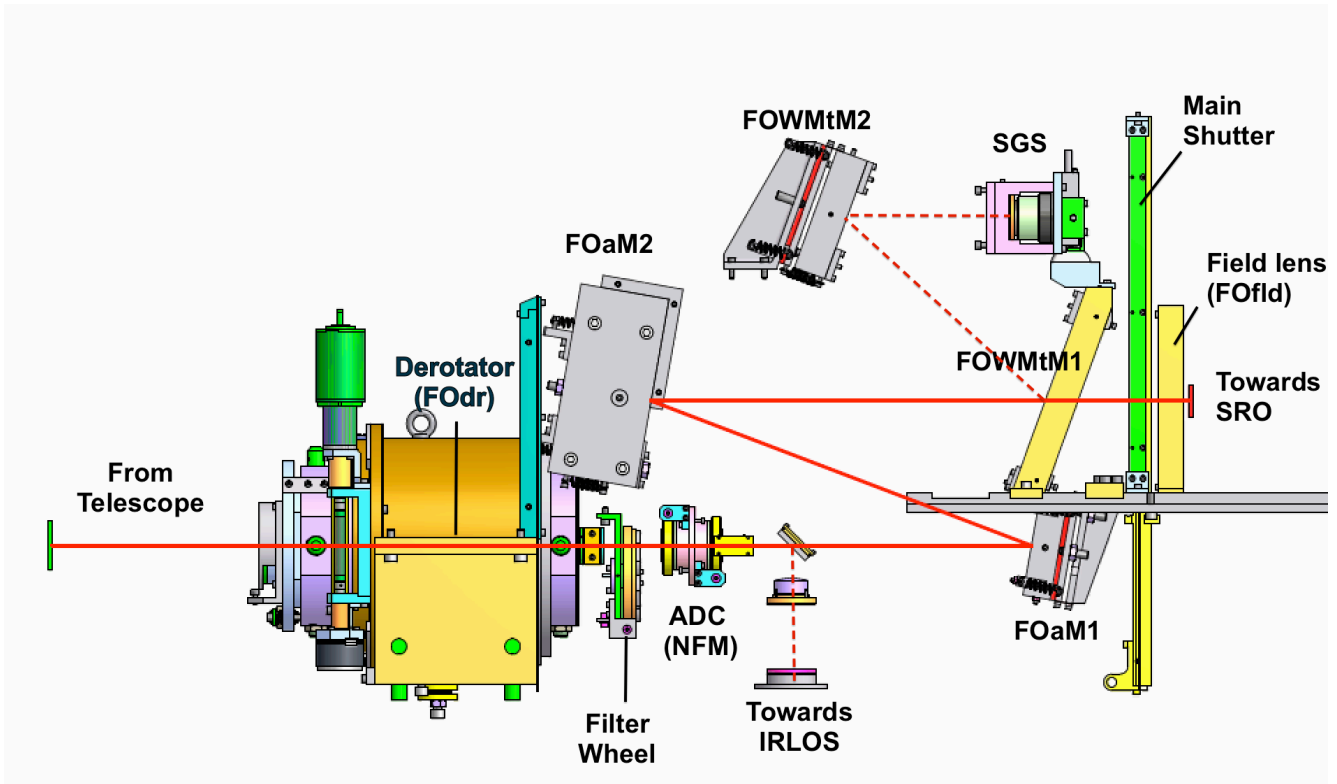


Figure 3: Schematic view of the subsystems in the Fore-Optics.



1.1.2.2 Fore Optics

The fore-optics system is shown in Figure 3. The top panel presents the optical elements (details in the text), and the bottom 3D view shows the path of light rays. It comprises the following subcomponents:

- **Derotator**

The derotator compensates for the field rotation at the VLT Nasmyth focus. It is a classical derotator based on two prisms: when rotated by an angle ψ , the image plane rotates by the angle 2ψ .

- **Filter Wheel**

A filter wheel is included in the fore-optics to adjust the spectral coverage according to the desired instrument mode:

- The nominal wavelength range of MUSE corresponds to 480-930 nm, which allows for suppression of second-order contamination in the red. In nominal mode, the blue cut-off filter is used to cut the wavelength range in the blue and avoid ghosts in that region.
- An “extended” wavelength range is available in WFM only, allowing observations down to 465 nm. However, strong second-order contamination appears in that case at $\lambda > 900$ nm (see Section 3.6 for details).
- In AO modes only, the range 584-594 nm is blocked to avoid contamination by sodium light from the LGS.

In total, 5 filters are available in the wheel. The relationship between instrument mode and filter name is provided in Table 8, Section 5.2.

- **Mode-switching unit and Atmospheric Dispersion Corrector (NFM only)**

The Mode-switching unit prepares the FOV when the instrument is used in NFM. It magnifies by 8 in each direction and includes the Atmospheric Dispersion Corrector (ADC). The ADC will be used, in NFM only, to correct for atmospheric dispersion. It consists in two Amici prisms working in counter-rotation.

- **IRLOS (NFM only)**

In NFM, a dichroic reflects the infrared light towards IRLOS, with the InfraRed Low Order Sensor measuring the wave front errors invisible to the LGS-AO system. It is a Shack Hartman sensor with 2 by 2 sub apertures working in the MUSE FOV at a wavelength range of 980nm to 1800nm. It senses image drifts occurring in NFM and corrects them by means of the AO loops.

- **Anamorphoser**

Two cylindrical mirrors (FOaM1 and FOaM2, Figure 3) provide a magnification of 0.5 to the beam in the horizontal direction within the fore-optics to ensure sufficient sampling in the dispersion direction.

- **Slow Guiding System (SGS)**

When in WFM mode, an elliptical pick-up mirror (FOWMtM1, Figure 3) separates the central FOV (corresponding to $1 \times 1 \text{ arcmin}^2$ on sky) from the four metrology fields surrounding it, which are reflected towards the WFM Slow Guiding System (Figure 3) after removing the magnification using the FOWMtM2 mirror. Incoming light is recorded by the SGS using a NACE 1k x 1k Technical CCD (having a 0.09" pixel scale). The system automatically detects astrophysical sources in the metrology fields of stacked exposures (Figure 4) and corrects for small motions by sending commands to the Telescope in a closed loop. These corrections are sent on average every 2 min. Therefore, in practice, the first offset sent happens after the second stacked exposure is recorded (i.e. 4 min.). The minimum and maximum brightness of stars useful for the SGS are approximately $R=21.5$ and $R=9.5$ respectively. Note that some useful parameters, such as image quality and transparency, are monitored by the SGS during an observation and saved in the FITS file of the science exposure as extension `SGS_DATA` (See Section 6.2)

Figure 4, left, shows the location of the metrology field used by the SGS, as seen on the detector¹. On the right there is an example of SGS image showing the detected stars used to monitor small motions (white squares). Note that the SGS image is flipped vertically when oriented on sky.

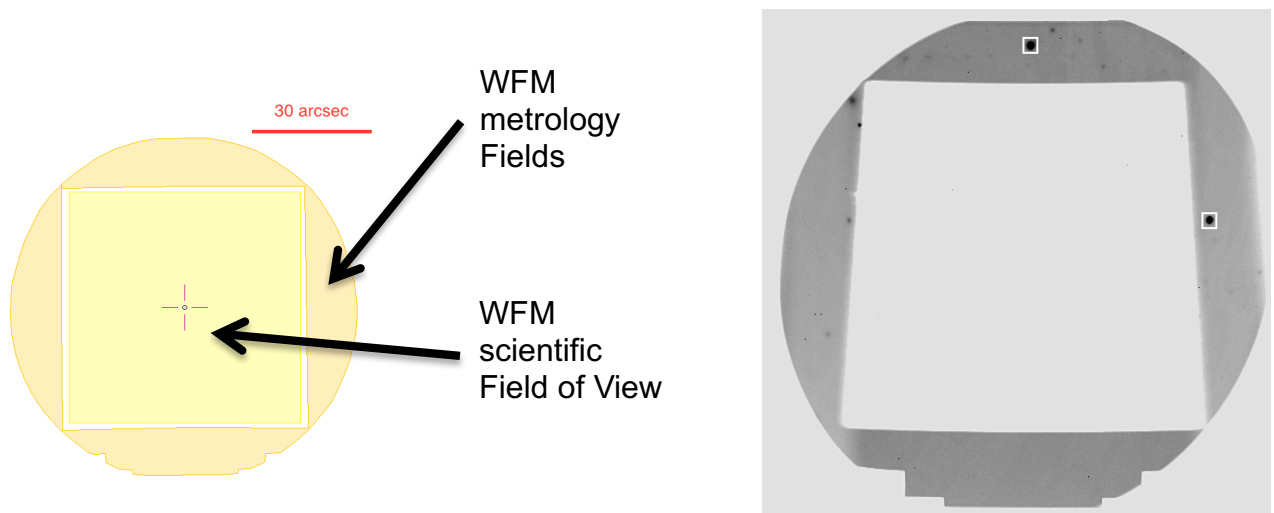


Figure 4: Slow Guiding System (SGS) metrology fields.

- **Exposure shutter**

This shutter is located between the SGS pick-up mirror (FOWMtM1, Figure 3) and the exit beam. It is a Bonn shutter with a rectangular aperture moving along the vertical direction. Shutter delay has been measured at 7.0-7.5 ms.

¹ Note that the SGS area was modified with the installation of GALACSI. The outer boundary of the metrology field is now set by the inner edge of the TTS annular pickup mirror in GALACSI. This annular mirror follows the pupil of the telescope and hence appears to rotate with respect to the MUSE science and metrology field-of-view. The metrology field shown on the left panel of Figure 4 represents the area that is accessible to the SGS in all configurations.

1.1.2.3 Splitting and Relay Optics (SRO) system

The SRO system splits the MUSE FOV into 24 channels and redirects the light of each channel towards the entrance of an IFU. It is composed of a field-splitter and a field separator, which separate the field into 24 horizontal beams (Figure 5). These sub-fields feed 24 relay optics, which correct for the variations in optical path from one channel to another (Figure 6).

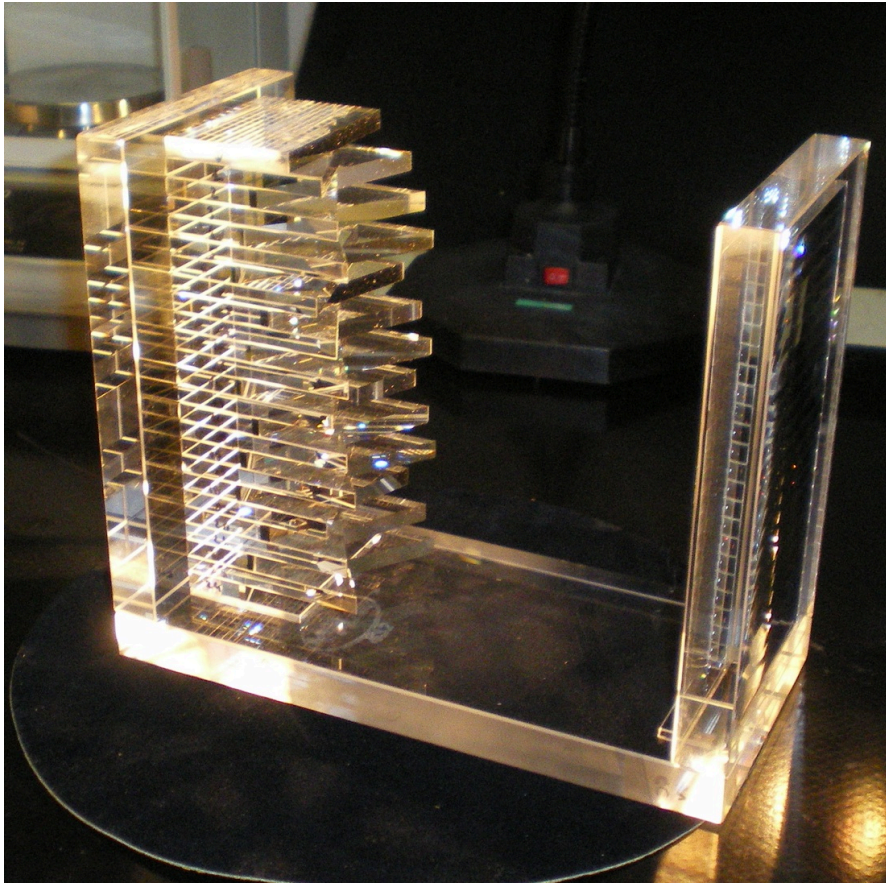


Figure 5: MUSE Field splitter and field separator optics. The 24 mirrors positioned at varying angles split the MUSE field-of-view in 24 horizontal bands.

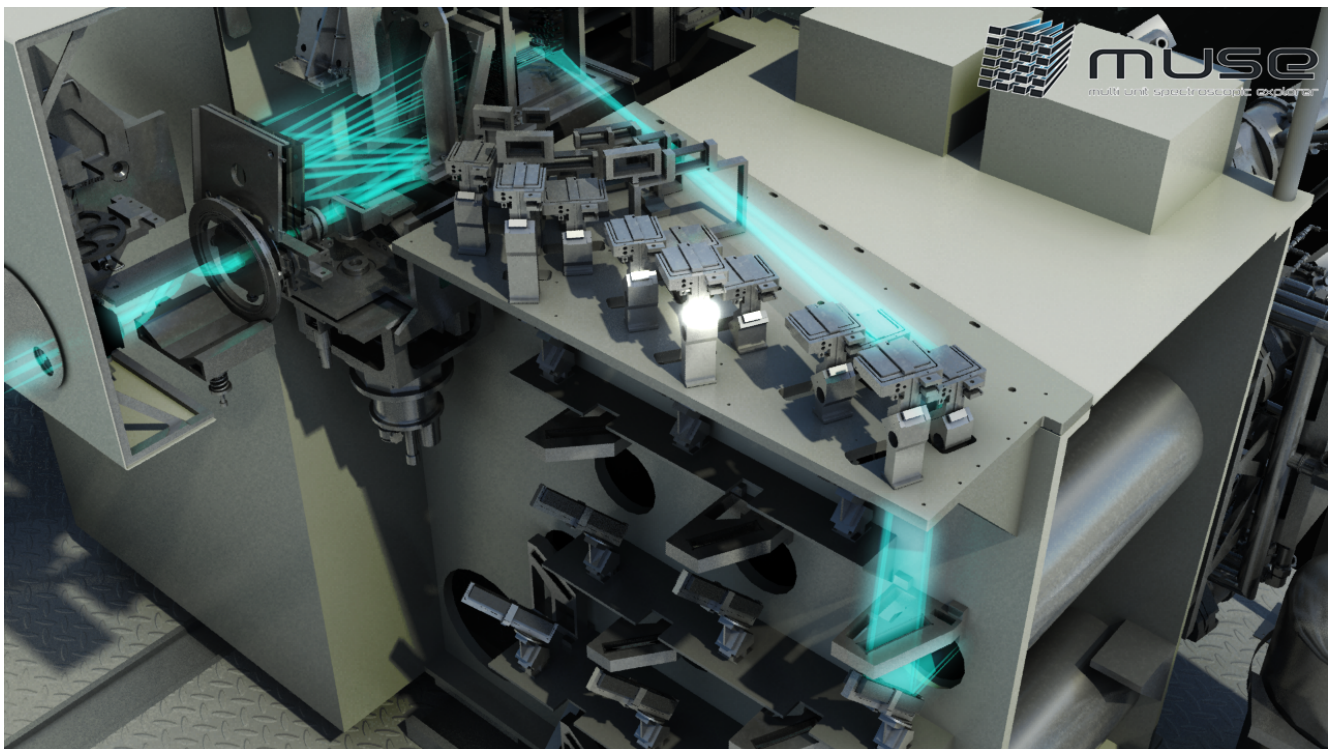
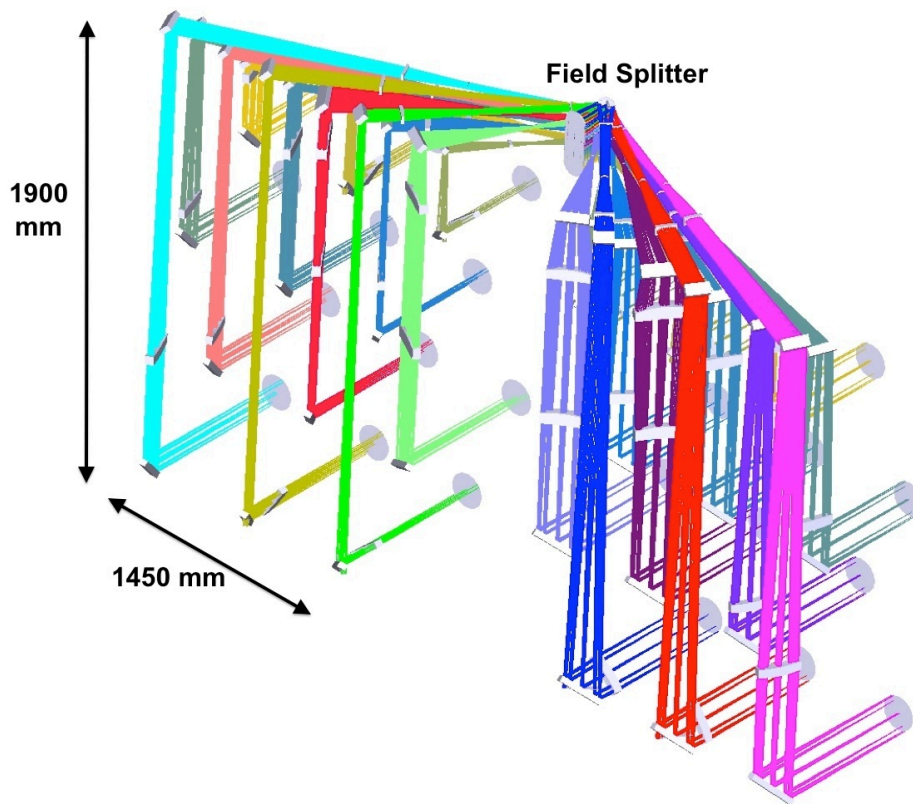


Figure 6: 3D view of optical paths for all channels due to the relay optics splitting of the field-of-view into 24 channels. The bottom figure shows the path of light rays for one of the channels, as seen from the Fore-Optics.

1.1.2.4 Integral Field Unit

Each of the 24 Integral Field Units (each assigned to a given channel) is formed by the combination of an image slicer, a spectrograph, and a detector, which we describe below. The optical layout of one of the IFU is presented in Figure 7.

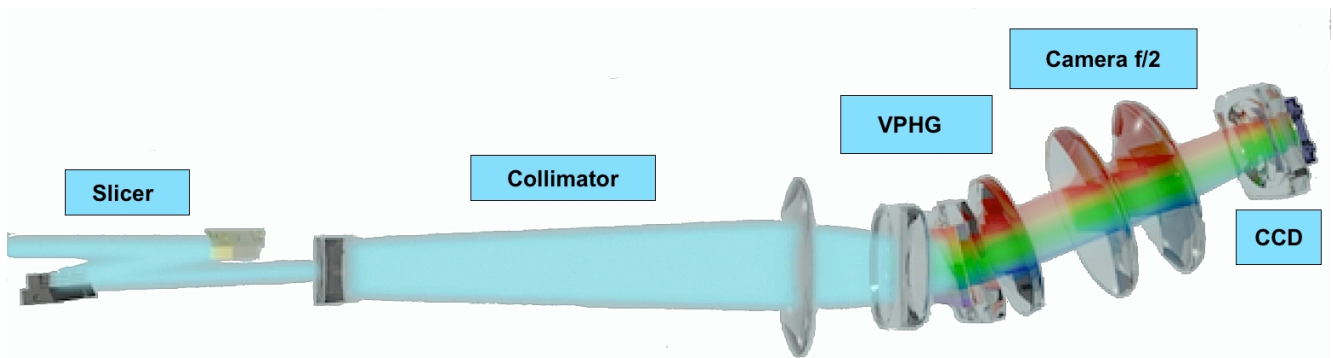
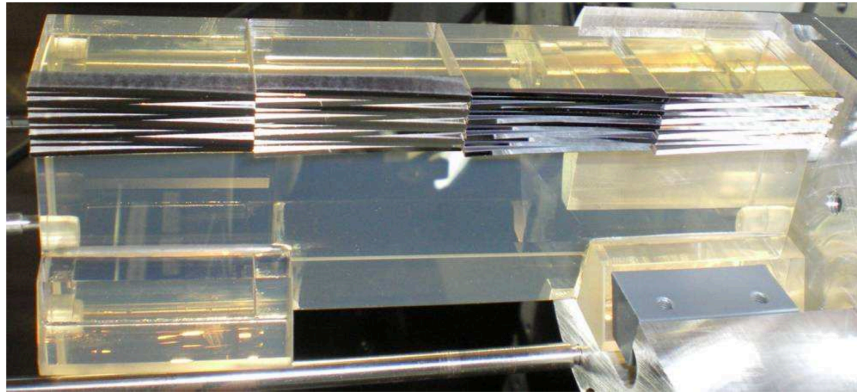


Figure 7: Overview of the optical layout for one of the IFUs. The top panel shows one of the slicers, which cuts the FOV of each channel into 4 stacks of 12 slices. The bottom panel shows the optical elements in the IFU and the path of light to the CCD.



1.1.2.4.1 Slicer

The slicer cuts and rearranges the 2D sub FOV in a 1D pseudo slit of 0.2" width. The main function of the image slicer is to slice the fraction of the FOV coming from the SRO into 48 slits that are rearranged in a long slit at the entrance of the spectrograph. The slicer is composed of:

- an image dissector array separating the beam in 48 slices (as represented on top of Figure 7)
- a focusing mirror array, which rearranges and aligns the slices
- a pupils/slits mask reducing scatter light and ghost images before entering the spectrograph.

1.1.2.4.2 Spectrograph

The main function of the spectrograph is to produce the spectra of the mini slits and image them onto a detector. It is composed of a collimator, a Volume Phase Holographic Grating and a camera. The grating disperses the mini slits in the perpendicular direction and achieves a spectral resolution of 1750 at 465nm to 3750 at 930nm (Figure 15). There is no moving part in the spectrographs and all 24 spectrographs are identical.

1.1.2.4.3 Detector

The light exiting each of the 24 spectrographs is sent onto a 4k x 4k, 15 μ m pixel CCD, operating at 163 K. The nominal characteristics of these detectors are given in Table 3.

Parameter	Value
CCD Type	E2V Deep depletion, AR graded coated
Active pixel format	4096*4112 pixels (X*Y)
Pixel size	15*15 microns
Pre-scan pixels in X direction	32
Overscan pixels	32
Detector gain	1.1 ADU / e-
Saturation	65000 e-
Linearity	<0.5% non-linear residuals
Binning factor	1x1 only
Readout noise	2.6 e-
Number of readout ports	4
Readout speed	100k pix.s-1
Readout time to RTD	40 sec
Dark current at 160K	3 e-.pix-1.hr-1

Table 3: Properties of the MUSE detectors.

The twenty-four scientific detectors of MUSE are controlled using four New Generation Controllers (NGC). The readout is always used without binning during observation.

The detector imaging area consists of four individually read quadrants of 2048 x 2056 pixels (X x Y) each, separated by pre-scan and over-scan regions. In the normal (science) readout mode, both pre-scan and over-scan regions have 32 pixels in size (Figure 8). Each quadrant is characterized by its own RON, gain, and bias level.

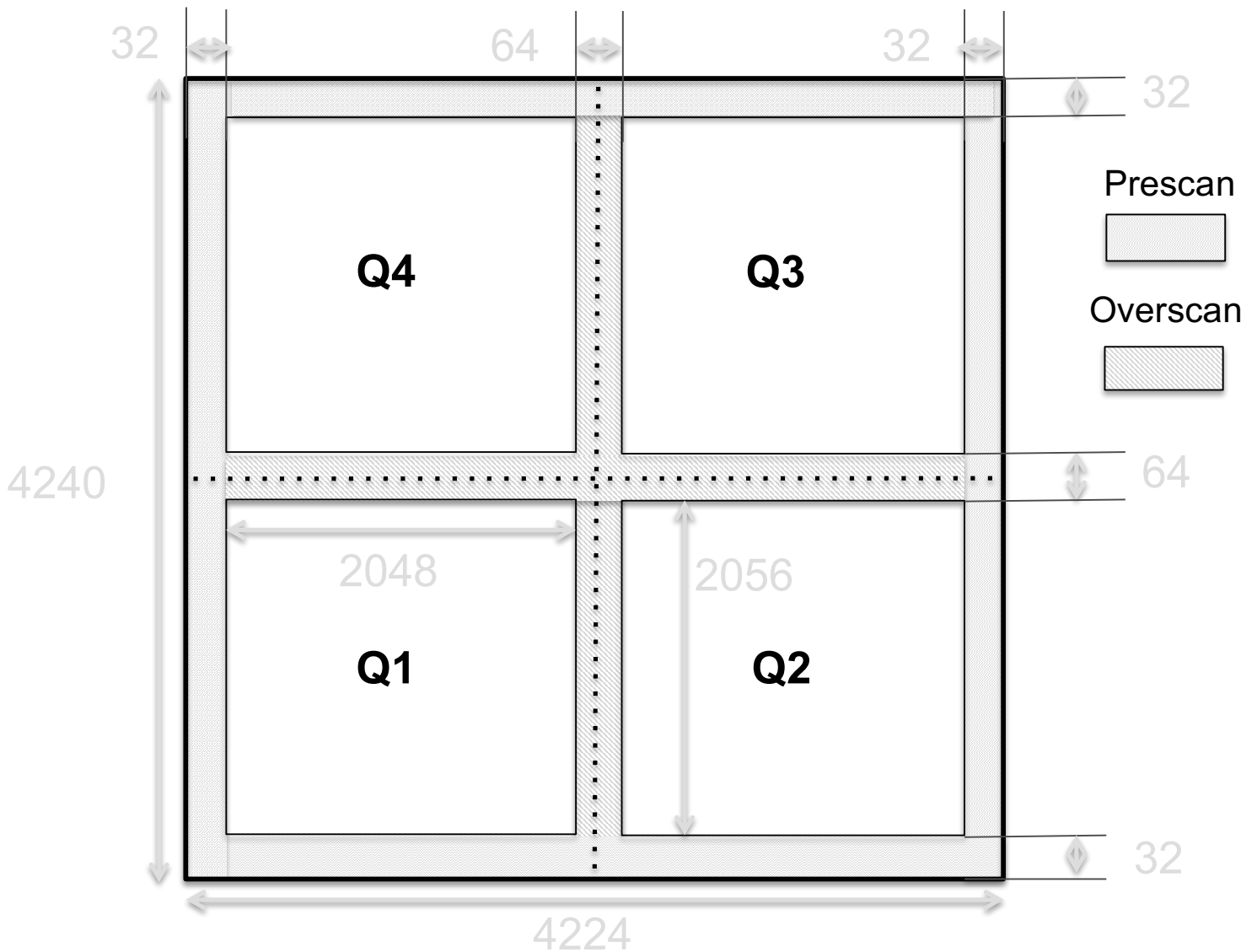


Figure 8: Overview of the pixel map of one for one of the detector, showing the 4 quadrants and the pre-scan / over-scan regions. All scales are given in pixels.

1.1.2.5 Spectral format

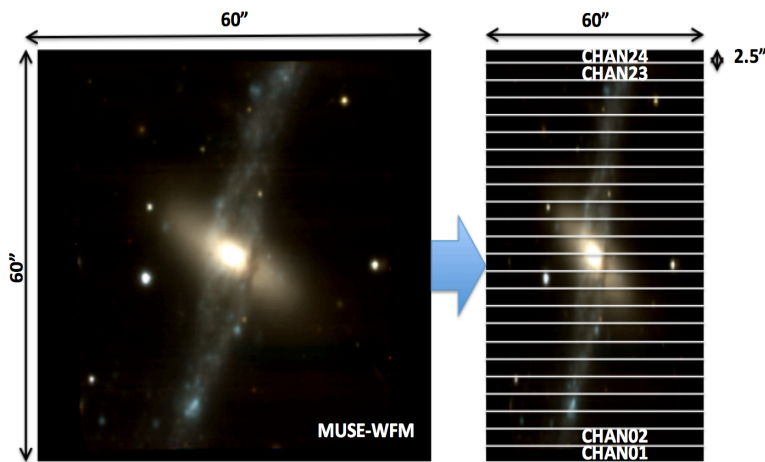


Figure 9: Overview of the splitting of the field-of-view from the fore-optics to one of the MUSE detectors. Left: splitting of the MUSE FOV into 24 sub-fields entering each channel. Center: shape of the entrance slicer on sky, with 4 stacks of 12 slices (numbered in red from 1 to 48) covering a 2.5 x 60" field. Bottom: location of each slice on the detector, with the corresponding wavelength range.

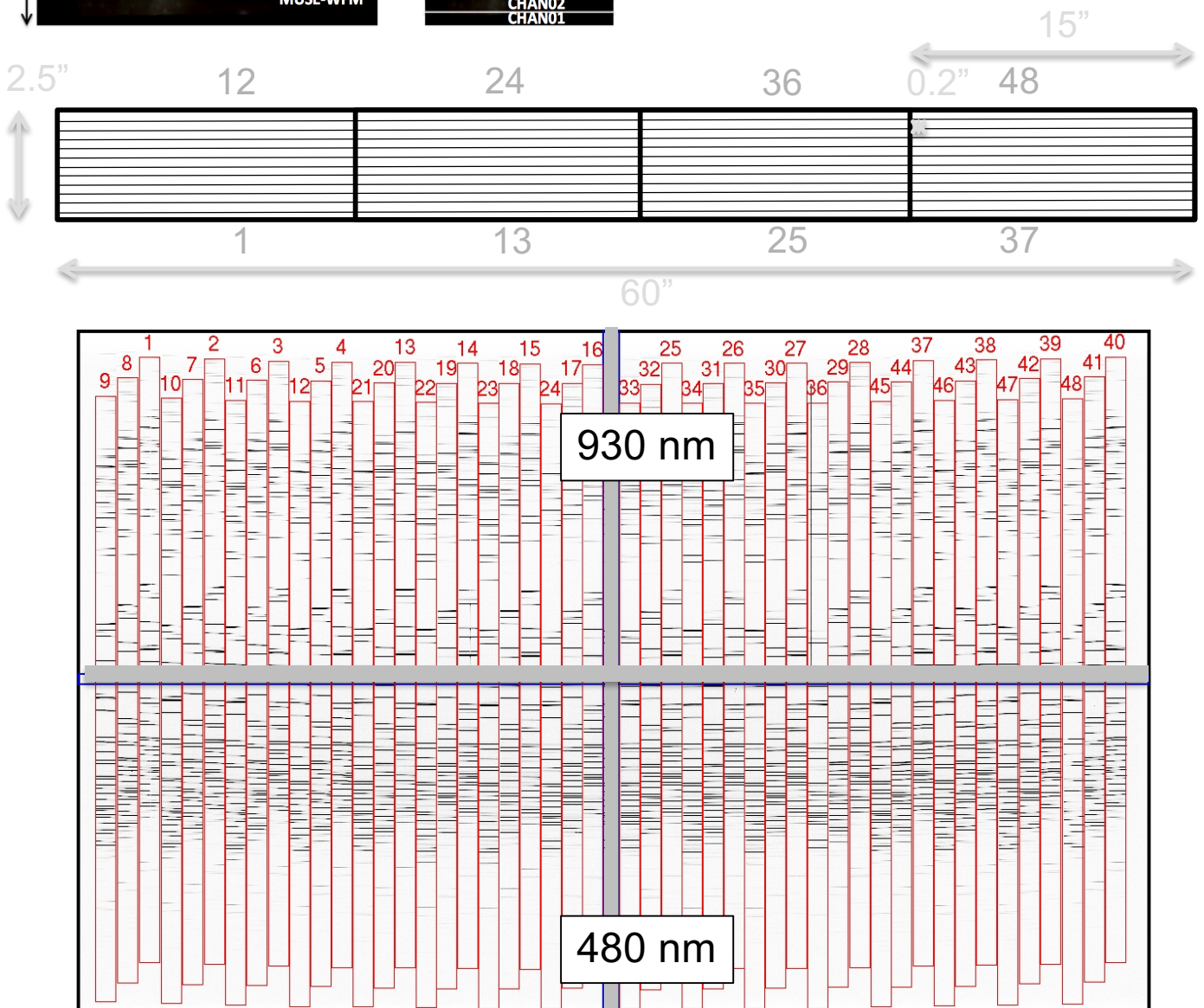




Figure 9 gives an overview of the spectral format as seen on one of the detector, and the relationship with the splitting and slicing of the field of view in the sky frame, when used in WFM. The spectral format is identical in NFM, except that the field-of-view is 7.5" x 7.5".

After splitting the magnified FOV into 24 sub-fields entering each of the 24 IFUs (top-left panel), the image slicer separates a sub-field into 48 slices (middle panel), and aligns them along the horizontal axis of the detector (bottom panel). The numbers 1-48 show the relationship between the image slicer mapping and the CCD mapping. Each slice is ~ 75 pixels wide, and dispersed in the spectrograph along the vertical axis of the CCD, with the bluest wavelengths located the bottom of the detector and the reddest wavelength at the top. The 48 slices are offset vertically from one another by ~ 125 pixels, following a repeating pattern of 3 slices.

1.2 Technical Description of GALACSI and the AOF

1.2.1 Overview of the Adaptive Optics Facility (AOF)

The ESO Adaptive Optics Facility consists in an evolution of the ESO VLT UT4 (Yepun) to a laser driven adaptive telescope with a Deformable Secondary Mirror (DSM) and four Laser Guide Stars (4LGSF). In addition, two Adaptive Optics wavefront sensing modules have been developed: GALACSI for MUSE described in this manual and GRAAL for Hawk-I.

1.2.1.1 The Deformable Secondary Mirror (DSM)

The DSM is the heart of the new facility. The design and manufacturing were done by Microgate and ADS (Italy). It implements all the VLT required functionalities plus the needed adaptive optics functions. 1170 force actuators are used to modify the shape of a 1.95 mm thick Zerodur thin shell (see Figure 11). Voice coils are attached to a cold plate that serves two functions: mechanical holding systems for the actuators and heat evacuation. The cold plate is also supporting the reference body: this piece of optics, made of Zerodur, is used as an optical reference and is facing the thin shell rear surface with a gap of almost 100 microns in between. Magnets are glued onto the thin shell applying the deformation when the voice coils produce a magnetic field. Metallic coatings deposited on the reference body and collocated on the thin shell form 1170 capacitive sensors that are used in an internal control loop to maintain the mirror at the proper shape. A picture of the full DSM assembly is shown in Figure 10.

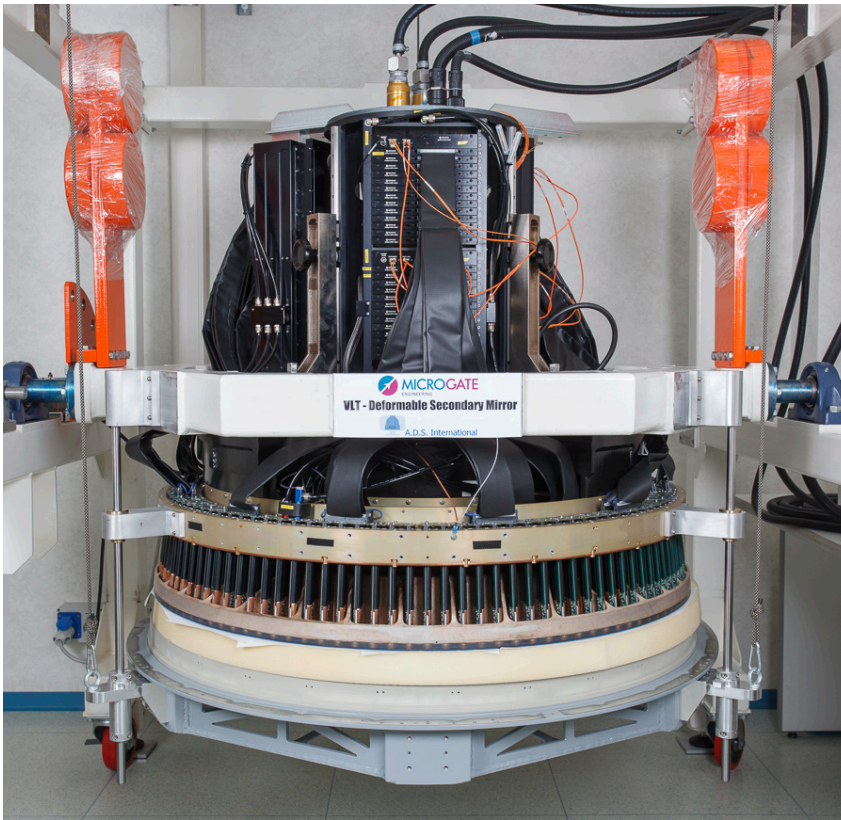


Figure 10: The Deformable Secondary Mirror on its test stand before shipping to Paranal.

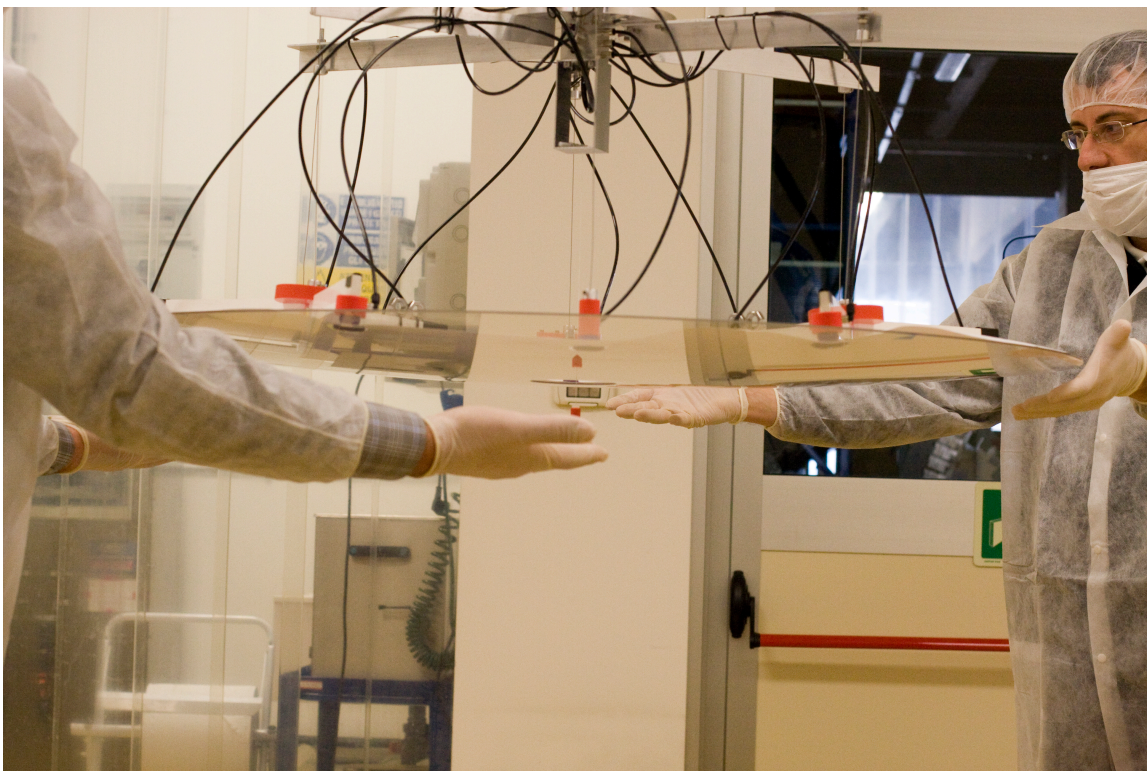


Figure 11: careful handling of the DSM 1.95mm thin shell during manufacturing.

1.2.1.2 The Four Laser Guide Star Facility (4LGSF)

Attached to the main structure of the telescope itself, the Four Laser Guide Star Facility (4LGSF, see Figure 12) provides all required hardware and software to launch the laser beams in the atmosphere. Each of the four laser units provides a 20 W beam launched through a 40 cm telescope. The laser design is based on a Raman Fiber Amplifier (RFA) technology first developed at ESO and subsequent frequency doubling realized by a Second Harmonic Generation resonant cavity. The laser also generates the Na D_{2a} and D_{2b} lines to promote back-pumping of the Na atoms and thus maintaining an efficient return flux for the wavefront sensors. Systems are compact and the lasers, plus beam diagnostic and launch telescopes are mounted directly on the telescope Center-Piece. The launch telescopes are x20 athermal beam expanders including only 2 single lenses with, in between, a 45deg steering mirror that can be tilted to point the beam at the appropriate location in a ± 6 arcmin field-of-view. At the entrance of each launch telescope, a fast tip-tilt mirror controlled at 1 kHz is used to correct for laser jitter. The 4LGSF also includes an aircraft avoidance system and interlocks to ensure a safe operation of the system.

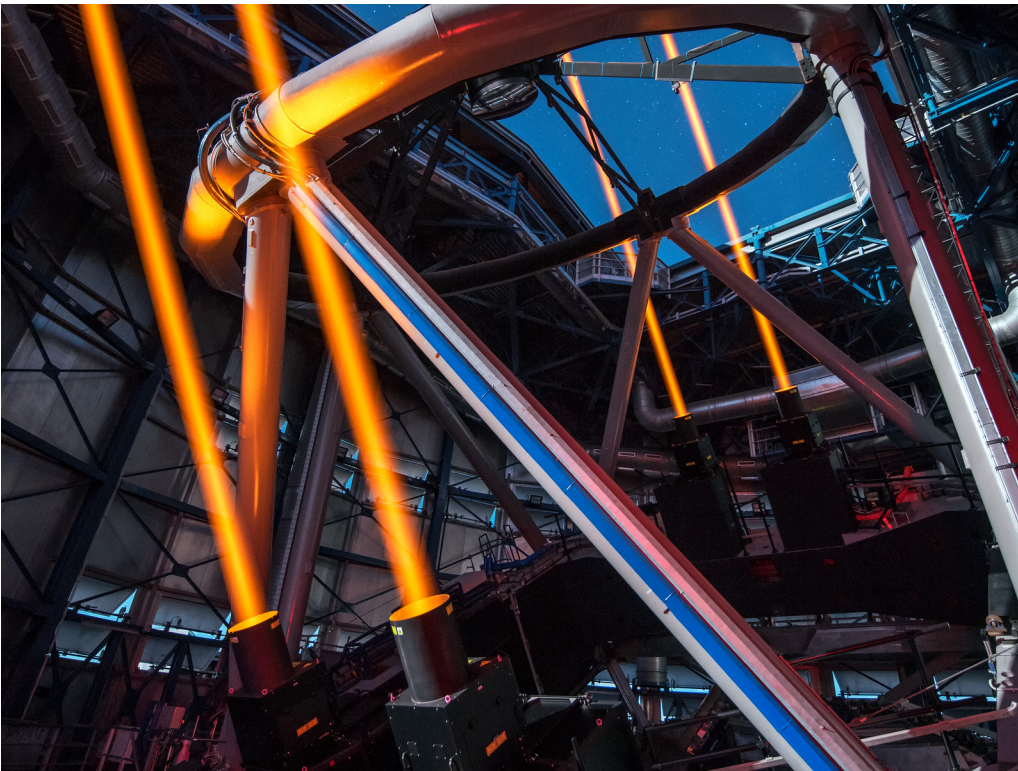


Figure 12: the 4LGSF in action

1.2.2 Overview of GALACSI

1.2.2.1 Wide Field Mode

The aim of the GLAO correction in WFM is to increase the ensquared energy (EE) within MUSE spatial pixels homogenously over the whole MUSE WFM field-of-view. In this mode, the four LGS are located at 64" off-axis i.e. outside the scientific field of MUSE. The visible Tip-Tilt natural guide Star (TTS) is located within a 3.5' technical field-of-view but outside the 1' field-of-view of MUSE. The

scientific beam path is not affected by any of the optical component within GALACSI (i.e. scientific beam simply goes through GALACSI).

The separation of the technical light path from the scientific beam path is done with an annular mirror located near the Nasmyth focal plane. It lets the central 1.4 arcmin of the field pass through towards MUSE and reflects the light towards the LGS and TipTilt Wavefront Sensor paths. By means of a Sodium (Na) Dichroic the LGS light is reflected towards the focus compensator, and a telecentricity lens. A reflecting pyramid sends then the four LGS beams towards their respective wavefront sensor paths. Each of them consists of a pupil re-imaging lens, a jitter actuator, and an additional pupil relay to create the pupil on the wavefront sensor lenslet array.

The LGS wavefront sensors measure the turbulence in each of the four directions. The beam overlap depends on the turbulence layer height and is largest for the Ground Layer. The reconstructor estimates the deformable mirror commands for each wavefront sensor and averages them before being applied to the ground conjugated DSM. The averaging of the DSM commands from each wavefront sensor has the effect that only the correlated part of the wavefront error is corrected being the one of the Ground Layer turbulence.

A sketch of the optical layout in WFM is presented in Figure 13.

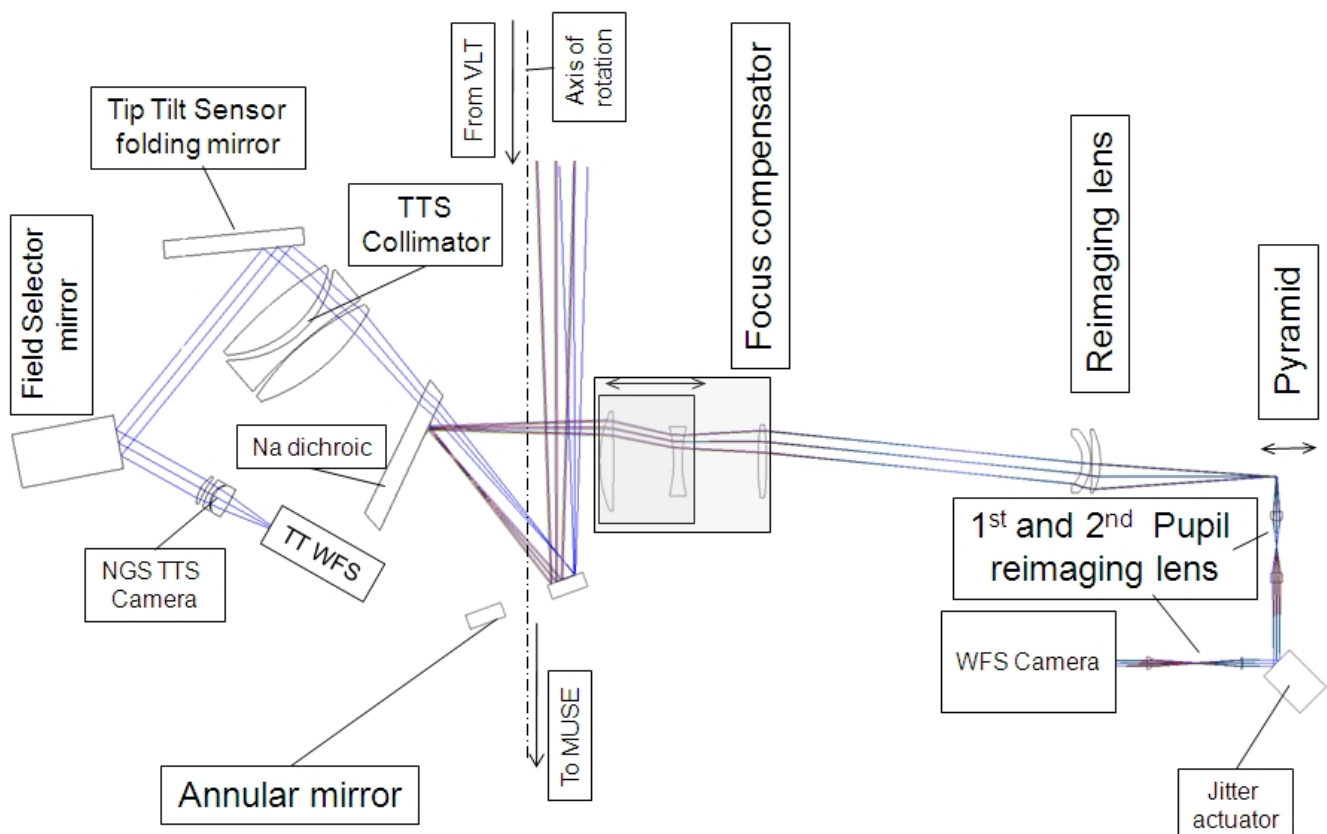


Figure 13: GALACSI WFM layout of the optical paths to the tip-tilt sensor and to one of the LGS wavefront sensor. The MUSE science beam runs unaffected along the axis of rotation.

1.2.2.2 Narrow Field Mode

[Not yet offered]

3 Overall performances and characteristics

3.1 Absolute throughput and limiting magnitude

The absolute throughput of the overall system (MUSE+UT4) has been measured by observing spectrophotometric standard stars during commissioning. The throughput in both modes peak to a high value >30% around 700 nm, and is overall > 15% (Figure 14). At shorter wavelengths, the throughput in the nominal mode (WFM-NOAO-N and WFM-AO-N) drops around 480 nm, while the extended mode gives a high throughput down to 465 nm. Note that in the AO modes, the wavelength around the NaD lines is blocked to avoid contamination and saturation of the detector by the strong laser light.

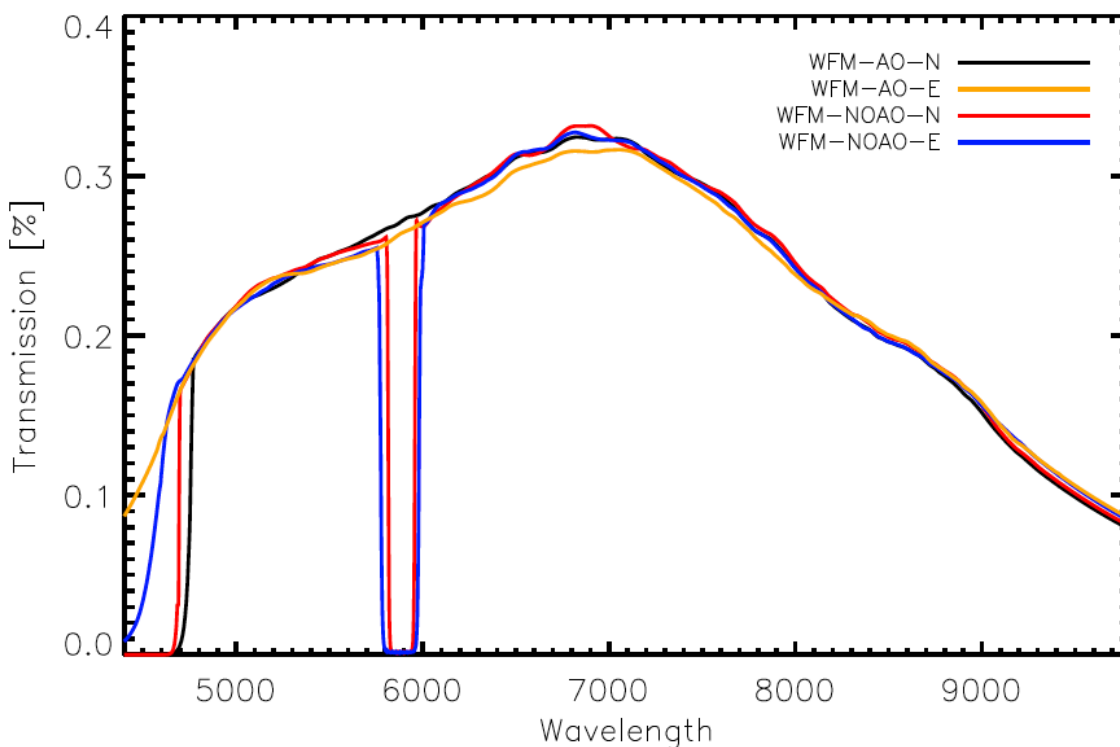


Figure 14: End-to-end MUSE+VLT/UT4 throughput, as derived from spectroscopic standard observations.

We have used this measured efficiency curve to predict the performances of the instrument in spectral continuum observations. We are assuming a 1 hour observation of a point source at airmass = 1.0 and a seeing of 0.8" in V. The limiting magnitude at S/N=10 per spectral resolution element, in regions free of sky lines, is reached for the following AB magnitudes (Table 4).



Filter	Wavelength	AB mag (S/N=10)
V band	550 nm	22.64
R band	640 nm	22.70
I band	784.9 nm	22.28

Table 4: Limiting magnitudes of MUSE per spectral resolution element.

Similar results for different sources/conditions, as well as more detailed performances, can be obtained using the dedicated Exposure Time Calculator available on the ESO website:

<http://www.eso.org/observing/etc/bin/gen/form?INS.MODE=swspectr+INS.NAME=MUSE>

3.2 Spectral resolution and sampling

In all instrument modes, the spectral resolution increases between 1770 at the bluest wavelengths (480 nm) and 3590 at the reddest wavelengths (930 nm). This was measured on wavelength calibration data (Figure 15). Each resolution element is sampled by 2.5 pixels along the spectral direction.

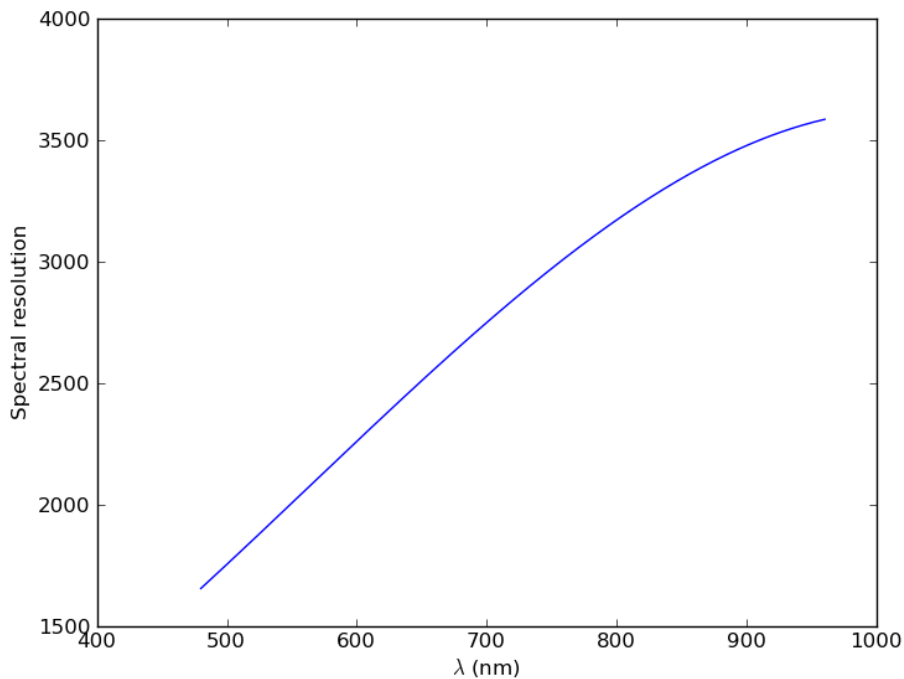


Figure 15: Spectral resolution achieved as a function of wavelength, as measured in the lab using calibration lamps.



3.3 Exposure timing

The performances of the Bonn² shutter have been estimated to provide an error $< 300 \mu\text{s}$ on the total exposure time. In addition, and due to the shutter mechanisms, variations in the exposure time across the FOV are possible, but have been estimated to be $< 1\text{ms}$ over the entire FOV. Recent measurements estimate the shutter delay at approximately $7.0 - 7.5 \text{ms}$, that is, to every exposure you should add 7ms to the value in EXPTIME header keyword to get the actual exposure time.

3.4 Overall illumination and uniformity

There are several factors that are decreasing the MUSE throughput in some specific area. The first factor is the Field Splitter: the gap between the Field Splitter lenses causes a small light loss that affects the 4 slices at the bottom and the 4 slices at the top for each channel. The gap is smaller than $50\mu\text{m}$ for a spaxel size of $580\mu\text{m}$, so the light loss is lower than **8.3%** for these channels. The effect is visible as horizontal regions of lower illumination in a continuum flat-field image (Figure 16).

The second factor is the gap between the 4 stacks of 12 slices in each channel that is $20\mu\text{m}$ for spaxel size of $465\mu\text{m}$ in this direction. The **4.3%** of light loss affects only the spaxels at the edges of the slices, and is visible as vertical regions of lower illumination in the continuum flat-field image (Figure 16).

Finally there is the geometrical shadowing of some slices by the neighbouring slices at the slicer level. In the worst case, there is **7%** of light loss. But integrated over the entire slicer stacks, the light loss is only **0.4% per channel**.

Very high SNR flat-field exposures obtained in the laboratory have been used to characterize the global illumination as a function of position (Figure 16). The median flux value is used as a reference to measure the flat-field variations. The main characteristics are the following:

- The small vertical distortion is visible as the global trapezoidal shape of the FOV: slices from the top channel have a larger horizontal extent than the bottom channel.
- In general, the flat-field is quite uniform, with variations of $\pm 2\%$ within a given channel / stack.
- At the top/bottom edges of each channel, a horizontal drop of $\sim 10\%$ in illumination due to the field splitter vignetting.
- In between the 4 stacks in each channel, there is a vertical drop of $\sim 30\%$ in illumination is visible, due to the inter-stack vignetting.
- A small flux variation ($\sim 2-3\%$) is visible between the central 2 stacks and the leftmost and rightmost stacks. This is predicted by design.

² Bonn shutters are travelling slit type shutters characterized by high exposure uniformity across the aperture. For more info see <http://www.bonn-shutter.de>

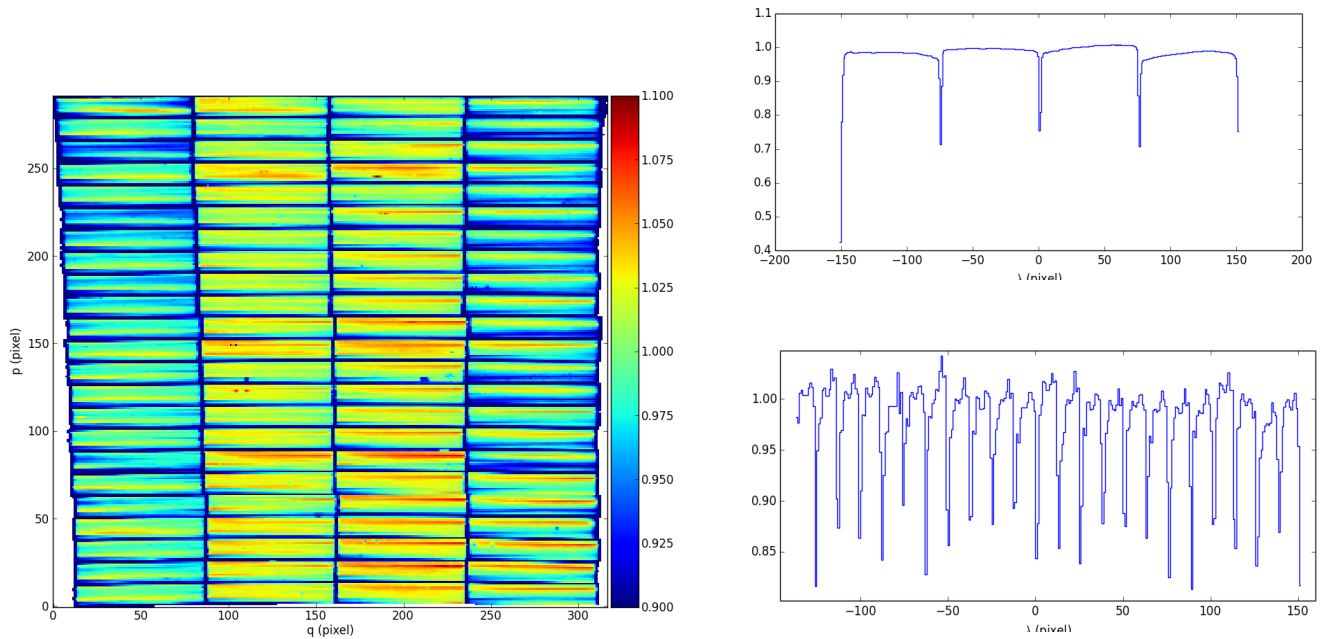


Figure 16: (left) normalized reconstructed image of the continuum flat-field in WFM. (right) horizontal (top) and vertical (bottom) cuts through the normalized image showing the horizontal and vertical variations in illumination.

3.5 Distortion and astrometric precision

The instrument distortion is calibrated by using a regular multi-pinhole mask as part of the overall calibration plan (see Table 11). The overall FOV of the instrument shows a trapezoidal shape (Figure 16), with channel 01 having a 3.5" smaller angular view in the horizontal direction.

The MUSE astrometric precision is calibrated on a regular basis by observing stellar cluster fields that have HST data of high astrometric quality. The astrometric solution has been obtained during commissioning-1 on these fields with an overall rms precision of 0.04" in each direction.

Astrometric precision is also calibrated on a regular basis by observing stellar cluster fields with a high astrometric precision. The astrometric solution has been obtained during commissioning 1 on these fields with an overall rms precision of 0.04" in each direction.

3.6 Second order contamination

In the **nominal** wavelength range (i.e. using the cutoff blue filter at 480 nm), the second orders appear, as expected, above the 930 nm wavelength limits (as shown as the red boxes in Figure 17). One can nevertheless see a faint contamination in the 920-930 nm region. In addition, the second orders are defocused and therefore extend beyond the slice. Because of their *3 steps pattern*, the slices extending higher on the detector are impacted by the adjacent second orders. The impact is nevertheless very limited.

In the **extended** mode (i.e. without any blocking filter), the impact of second orders is significant and starts already at **790 nm**. The contamination reaches levels of **~12%** at wavelengths redder than 850 nm.

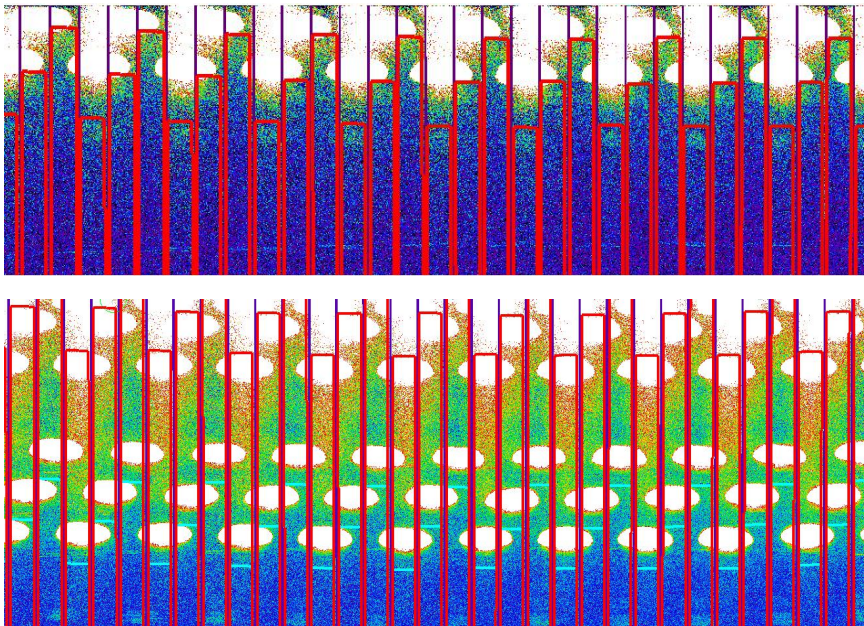


Figure 17: Second order effect in nominal (top panel) and extended (bottom panel) modes, shown here for a bright exposure with arc lines. The red boxes mark the slice limits up to 930 nm. The impact of second order is visible as the white ellipses illuminating the top of the detector. The nominal instrument mode is not affected by contamination, but it is more significant in the extended instrument mode.

3.7 Image Quality Gain in WFM AO

Ground layer adaptive optics correction essentially acts like a seeing enhancer allowing for good to excellent image quality a larger fraction of the time. By essence, the magnitude of the correction and the ability for the system to increase the energy in a spaxel highly depends on the turbulence profile of the atmosphere. The more the turbulence arises from layers close to the ground, the better the correction is. The target performance of GALACSI is to increase the energy ensquared in a 0.2"x0.2" spaxel of MUSE by a factor of two compared to natural seeing limited images when more than half of the turbulence is concentrated in the first 900m above the telescope. The fraction of the time with a dominant ground layer turbulence is still poorly known, therefore we cannot yet provide image quality improvement statistics. Note that this Ground Layer correction is by no means aimed at providing close to diffraction-limited images.

At the time of writing of this Manual, the instrument is still in the commissioning phase and performance of the Ground Layer Adaptive Optics under different atmospheric conditions is being assessed.

3.8 Maximum airmass of observation in AO mode

Due to the operational range of the deformable secondary mirror, the maximum allowed airmass for AO observations is 1.9.



3.9 Instrument stability

We present here some of the results on instrument stability, as known at the end of Commissioning 1. Two kinds of instabilities have been observed. The first one affects the detector system in the form of varying bias structure, difficult to subtract. The second one is a temperature dependent flat-field effect. The former instability has been very much reduced by improving the detector hardware and the introduction of a new continuous clocking scheme introduced after 19 July 2015. The latter has been addressed by the use of illumination frames taken several times during the night.

The long-term stability of the instrument is still being monitored, and the details in this section will be updated continuously with new findings.

Wobble:

The MUSE derotator produces a residual mechanical wobble, which produces a repeatable pattern as a function of the derotator position. When the instrument is used in WFM, the effect of this wobble will be compensated by the SGS.

When the SGS is not available (e.g., no suitable stars in the metrology fields), the impact of this wobble was estimated for the worst case of a 1 hour observation of a target close to the zenith (4 deg. Zenithal distance). We can reach a total displacement of 0.28", which has an impact of 10% on image quality in good observing conditions (0.6" seeing). In most cases, the impact will be much smaller.

Thermal stability:

MUSE has been submitted to thermal tests in the lab to assess its stability with regards to the ambient temperature. The resulting displacements in the spatial and spectral directions are provided in the Tables below. To predict the effect of temperature changes on observations we have used the Paranal statistics that give the median and peak temperature variation (ΔT) for various periods (1 hour, 1 night, 1 season, see left columns in Table 5 and Table 6).

The stronger impact appears in the wavelength direction. During 1 hour exposure the inferred motion is still small (<0.05 resolution element) and the impact on the LSF is negligible: e.g. assuming a Gaussian shape its FWHM will increase by a maximum of $(1+0.03^2)^{1/2} = 1.0004$, i.e. 0.04%. During 1 night, the offset is larger and can reach 0.4 Å. However it is always possible to use bright sky emission lines to correct for this offset. This is currently implemented in the sky subtraction pipeline recipe.

Table 5: Thermal stability in the spatial direction.

Conditions	Maximum offset in spaxel
1 hour median ΔT (0.5 °C)	0.01
1 hour peak ΔT (1.5 °C)	0.03



Table 6: Thermal stability in the spectral direction.

Conditions	Maximum offset in Å	Maximum offset in resolution element
1 hour median ΔT (0.5 °C)	0.06	0.03
1 hour peak ΔT (1.5 °C)	0.19	0.08
1 night median ΔT (3.2 °C)	0.42	0.17
1 night peak ΔT (6.0 °C)	0.78	0.31
Seasonal median ΔT (7.0 °C)	0.91	0.36
Seasonal peak ΔT (20.0 °C)	2.60	1.04

4 Problems to be aware of

4.1.1 Ghosts, straylight, spikes and ferris wheels

Ghosts : a ghost analysis has been performed on the detectors when illuminating the slices with bright saturated emission lines. The only detected ghosts have been observed at a very low level (<0.001%).

Straylight : similarly, contaminating straylight appears at a very low level ($< 10^{-5}$) when illuminating a channel with a very bright light source. This effect is seen at the level of the detector, with a background affecting the neighbouring slices.

Ferris Wheels : Observing close to bright sources with MUSE leads to the presence of strong artefacts within the datacube in the form of concentric rings, similar to a ferris wheel, and bright spikes. Typically these effects are seen when observing within a few arcminutes of a bright source.

Analysis of all these issues is still preliminary at this stage, and will be updated after a full analysis has been completed and the origin and solutions have been determined.

4.1.2 Remanence

The remanence of the detectors has been measured by performing long dark exposures shortly after a saturated exposure. Remanence measured in these dark exposures is very low (0.04 ± 0.23 e-) and its effect can be ignored.

4.1.3 Detector defects

Fringing: The choice of detectors for MUSE keeps the effect of fringing to a very low level. Fringing is apparent on very high signal-to-noise flat-field exposures in the 750-870 nm wavelength range, and is measured at a peak-to-peak level of 0.3% in WFM and 0.6% in NFM (Figure 18).

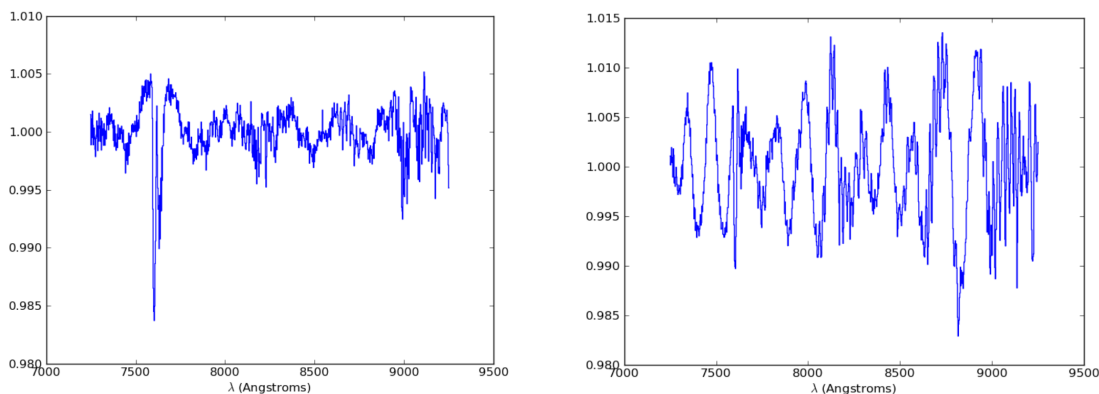


Figure 18: Fringing measured in the red, measured on normalised flat-field frames. (left) WFM, (right) NFM.

4.1.4 Bad columns/pixels

The MUSE detectors are generally of high quality, with only very limited regions of bad pixels. 17 out of the 24 detectors do not show any strong defect automatically flagged by the pipeline as a data quality (DQ) issue, and the remaining 7 detectors show between 1 and 3 bad columns. The full details of bad pixels flagged are given as reference for each detector in Figure 16 in Section 8.1.

4.1.5 Contamination caused by Na Laser during AO observations

During the first commissioning run of MUSE+GALACSI the commissioning team discovered that the upstream beam of photons induced Raman scattering with the air molecules leading to the presence additional lines sifted to the red of the main Na line. The spectrum seen by MUSE is contaminated by these lines to the extent shown in Table 7, and Figure 19 below. It is to be noted that the strength of the two brightest lines, those of N₂ and O₂, are comparable with a bright skyline. The MUSE commissioning team is working to define strategies to subtract them in the data reduction pipeline. For details see Vogt et al., Phys. Rev. X 7, 021044 (2017).

Table 7 Raman Lines visible with MUSE with laser on.

Raman Line	λ_{4LGSF}	CO ₂	CO ₂	O ₂ ($\nu_{1\leftarrow 0}$)	N ₂ ($\nu_{1\leftarrow 0}$)	CH ₄	O ₂ ($\nu_{2\leftarrow 0}$)	H ₂ O	N ₂ ($\nu_{2\leftarrow 0}$)
Raman shift (cm ⁻¹)	...	1285.8	1388.1	1556.4	2330.7	2914.2	3089.2	3651.7	4631.2
λ_{obs} (Å)	5889.959	6372.57	6414.39	6484.39	6827.17	7110.43	7200.02	7503.93	8099.23
Flux	1.9×10^7	11.3	18.9	6.8×10^3	2.0×10^4	≤ 1.1	3.2	2.7	16.1

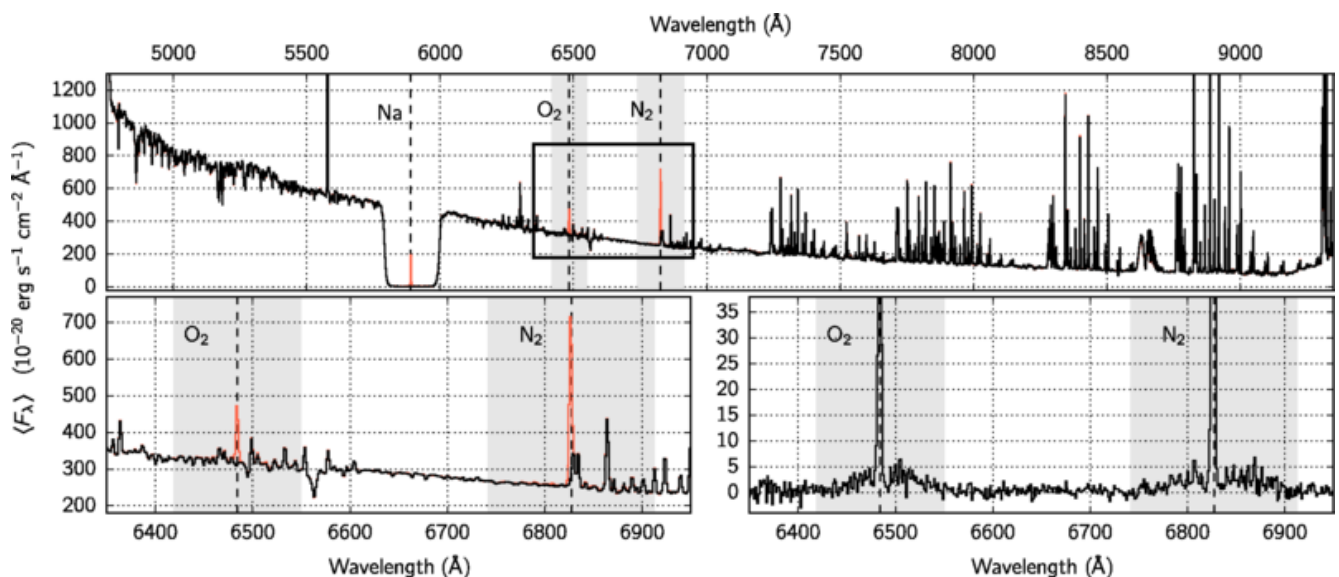


Figure 19 Sky spectrum seen by MUSE with 4LGSF on in WFM-AO mode.

4.1.6 Regions of reduced sensitivity on flat fields

MUSE flat field images for all channels show regions of lower transmission of varying strengths, which is believed to be due to dust on the field splitter. These regions stretch the full length of the spectrum, and appear as small spots on the reconstructed flat fields, as shown in Figure 19

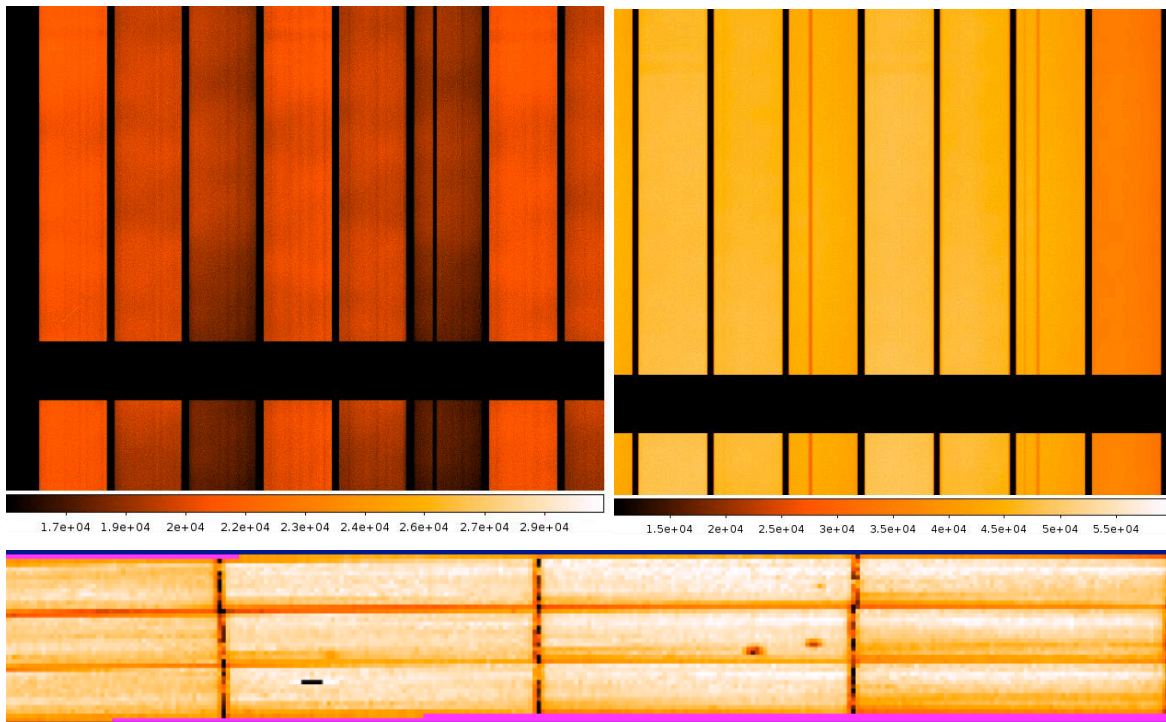


Figure 20: Dark features in the MUSE flat fields due to dust in the field splitter. Top: the regions of low transmission extend the full length of the spectrum. On the left is an N-mode flat and on the right is an E-mode flat. Bottom: the 'spots' of low transmission in a reconstructed datacube.



5 Observing with MUSE

5.1 General information

As for all ESO instruments, the P2PP software is used to prepare MUSE observations in Service Mode. The generic guidelines for Phase 2 and the P2PP software that can be found at the following links:

<http://www.eso.org/sci/observing/phase2/SMGuidelines.html>

<http://www.eso.org/sci/observing/phase2/P2PP3.html>

As of April 2017, all OBs for MUSE observations in Visitor Mode must be created using the new web application p2. The main differences between P2PP and p2 are that p2 allows the User to create OBs in a web browser, which are then recorded directly in ESOs database instead of the Users local cache. This use of the database eliminates the need to export/import OBs ahead of the observing run.

<https://www.eso.org/sci/observing/phase2/p2intro.html>

In service mode, the User shall provide during Phase 2 the OBs containing one acquisition and observation templates, fill the README information, and provide the corresponding finding charts following the rules given at

<http://www.eso.org/sci/observing/phase2/SMGuidelines/FindingCharts.html>.

As of P100, Users can also use the unified GuideCam Tool to create ESO compliant finding charts. The unified GuideCam Tool is a dedicated software that lets the User visualise the instrument field-of-view on sky, define the pointing and offsets, select guide stars and create finding charts. It can directly interact with P2PP (version 3.4.2 or higher) and p2 in order to attach finding charts or to propagate acquisition template parameters, such as guide star coordinates, to the OB.

https://www.eso.org/sci/observing/phase2/SMGuidelines/GUCT_generic.html

To help with MUSE preparation, we have created a MUSE-FOV template to use with ds9. One can create such a template by copying/pasting the code provided in Section 8.4.

Questions on Phase 2 preparation for service mode observations should be addressed to the ESO User Support Department (usd-help@eso.org)

5.2 MUSE Observing modes

MUSE has two basic modes: WFM for surveys and general use offered both with and without AO, and NFM with AO only [not yet offered] for achieving unprecedented spatial resolution across a sizeable field. Note that in AO mode the maximum airmass of observations is 1.9.

In addition there are two choices of wavelength range - the nominal (N) mode, which suppresses the 2nd-order overlap of blue light at red wavelengths (see Section 3.6), and the extended (E) mode, which does not use the blue cut-off filter and thus extends into the blue but suffers from the 2nd-order contamination redwards of 850 nm. The available instrument modes (WFM-NOAO-E, WFM-NOAO-N, WFM-AO-E and WFM-AO-N) are presented in Table 8, as well as the three additional instrument modes, which are expected for the future.



MUSE instrument mode	Spatial setting	Filter name	Spectral range (nm)
WFM-NOAO-N	WFM	Blue	480-930
WFM-NOAO-E	WFM	Clear	465-930 ^(*) with 2 nd order contamination at 850-930 nm
WFM-AO-N	WFM	Blue-Na	480-582, 597-930
WFM-AO-E	WFM	Na	465-578, 599-850 ^(*)
NFM-AO-N	NFM	Blue-IR	480-930 Nota: Na Notch in Galaxsi

Table 8: Summary of instrument modes, filter names and spectral ranges. Only WFM instrument modes are available at the moment, with one additional Narrow Field mode expected in the future (hatched). (*) See Section 3.6 about 2nd order contamination in the red for WFM-NOAO-E and WFM-AO-E instrument modes.

5.3 MUSE Target acquisition

The first template to be included in the OB is the **acquisition template**. For both seeing limited instrument modes (WFM-NOAO-N and WFM-NOAO-E), the template to be used for acquisition is **wfm-noao_acq_movetopixel**. For both WFM-AO instrument modes (WFM-AO-N and WFM-AO-E), the template to be used for acquisition is **wfm-ao_acq_movetopixelLGS**.

For WFM-NOAO case only, when no interaction/centering is needed a simplified acquisition **wfm-noao_acq_preset** can be used. In particular, this template should be used when a target centring accuracy of the order of 2"-3" is acceptable. In addition, the template **wfm-noao_acq_presetRRM** must be used for an acquisition OB in Rapid Response Mode. This latter template is an exact copy of the normal preset template with the addition of two hidden (from the user) keywords for bookkeeping and logistics.

The main parameters of the acquisition templates are the following:

- Instrument Mode
- WCS position of the FOV center (RA,DEC)
- Position Angle on the sky (measured from North through East). The convention for position angles with respect to the FOV is detailed in Figure 21.
- (*Optionally*) Position and magnitude of the VLT Guide Star. The VLT Guide Star must be between R band magnitudes 8 and 12 (in Vega), and located within the VLT guide star area (Table 9)

Providing the VLT guide star is not mandatory but is useful when combining observations taken at different days or when doing mosaic observations with MUSE. The quality of the astrometry in the headers of the raw data depends directly on the quality of the astrometry of the guide star.

- **For AO acquisition only**, position and magnitude of the AO tip-tilt star (TTS) with the possibility to provide an alternative TTS (optional but highly recommended) to mitigate potential difficulties during the acquisition sequence due to inaccurate TTS parameters (e.g. high proper motion star, double star, wrong magnitude...). **TTS star magnitude must be between R=6 and R=18.5**. In addition, note that:
 - o **the TTS must be chosen such that it remains in the TTS patrol field defined in Table 9 for all OBJECT positions in the subsequent observing template;**
 - o **Differential tracking is not possible with WFM-AO observations.**
- Exposure time of acquisition exposure. Typical integration times vary between 10 sec. (if there is a $V < 17$ point source in the FOV) and 2 min. (when the brightest point source is $V < 20$). If there is a need of precise ($< 1''$ error) pointing in fields where only faint extended sources are present, blind offsets are recommended.
- (*Optionally*) Blind offsets. The user has the possibility to apply some offsets with respect to a bright reference star centered in the FOV of MUSE, in case no bright source is visible in the FOV for direct acquisition and precise pointing is necessary. The convention is to provide telescope offsets (arcsecs in RA and DEC) to **move the telescope from the target to the reference star**.

$$RA_REFSTAR = RA_TARGET + \Delta RA$$

$$DEC_REFSTAR = DEC_TARGET + \Delta DEC$$

In that case, the sequence is the following:

- o The telescope points to the reference star by including offsets from the target
 - o The reference star is centered in the MUSE FOV.
 - o The offsets are cancelled and the telescope moves to the target position.
 - o For those familiar with the instruments, this definition of blind offsets is identical to the one used for HAWK-I and CRIRES.
- Slow Guiding (True/False): The use of the SGS is strongly recommended whenever individual exposure times on the science targets are larger than 4 min. The SGS will acquire a reference image and detect guide stars after acquisition, then lock on these stars and correct for small motions such as derotator wobble, which is important for long exposures, in particular close to the zenith. The user does not need to provide secondary guiding stars in acquisition, these are automatically found by the system. If all individual exposure times are shorter than 4 min., the user has the option not to use SGS because no correction will be sent to the telescope (see Section 1.1.2.2). Do not activate the SGS if you do differential tracking.

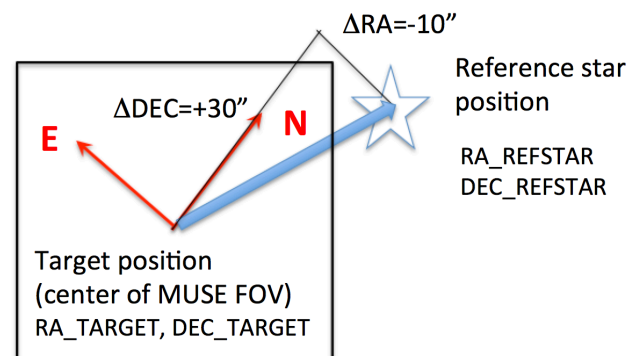


Figure 21: Convention for blind offsets during acquisition.

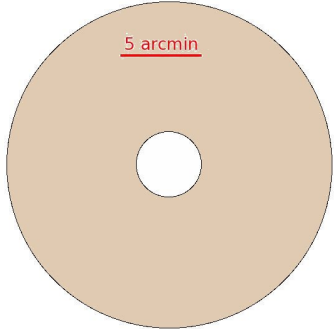
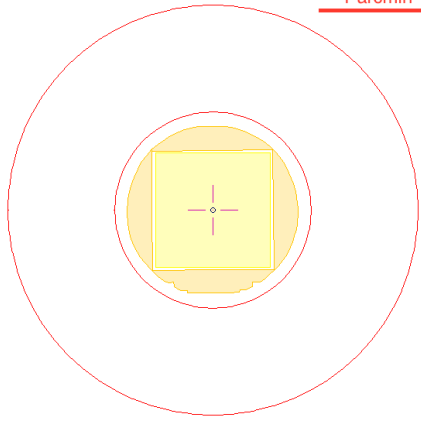
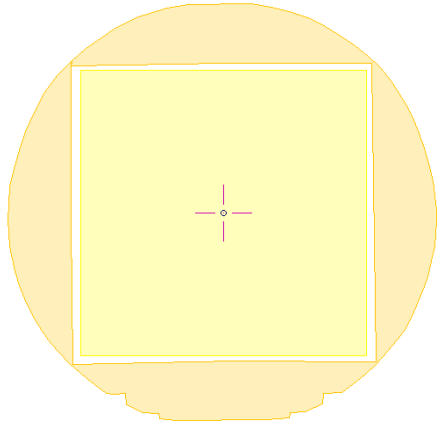
	Guide Star Area	Shape
VLT guide star	10 arcmin radius circle inside the unvignetted Nasmyth FOV 4 arcmin diameter circle excluded	
AO TTS	Between 1.725 and 3.59 arcmin diameter from the MUSE field center (covered area: 7.8 arcmin ²)	
SGS guide stars	SGS metrology fields, ~ 1.5arcmin square field, MUSE FOV excluded	

Table 9: Description of the different guide stars used for acquisition, and their corresponding region of sky with respect to the centre of the MUSE FOV



5.4 MUSE science observations

There is only one science template in both WFM-AO modes (WFM-NOAO-N and WFM-NOAO-E), **MUSE_wfm-noao_obs_genericoffset**, and one science templates for both WFM-AO modes (WFM-AO-N and WFM-AO-E), **MUSE_wfm-ao_obs_genericoffsetLGS** allowing the user to perform observations including a sequence of telescope and PA offsets, which is the recommended strategy for MUSE. It has been found that by rotating the instrument by +90, +180 or +270 degrees between exposures compared to the PA of the first exposure, the patterns of the slicers and channels (which appear as throughput variations in the flat-field image; see Figure 16) can be averaged out. The combination of a small dithering pattern (with offsets typically smaller than 1 arcsec) and 90 degrees rotations is currently the best strategy to reject cosmics, and get a more uniform combined dataset in terms of noise properties.

The science template allows the user to perform a number of exposures and offset the telescope and/or the instrument derotator to adjust pointing and PA in between each offset position. In addition, the user should specify the type of exposures: "O(BJECT)" or "S(KY)" within the specified offsets list. The science mode of MUSE to be used for this OB, as defined in Table 8 (e.g. WFM-NOAO-N), has been defined in the corresponding acquisition template in P2PP.

Important note for WFM-AO observations: users should verify that the TTS chosen in the acquisition remains within the allowed TTS area defined in Table 9 for all OBJECT positions. This constraint does not apply to SKY positions because during SKY observations, the tip-tilt loop is open and only the high-order correction with the LGS remains active. Note also that there is no particular additional constraint on PA offsets with AO.

The total number of exposures performed is the combination of two parameters: NOFF (number of offsets read in the list, see below) and NEXPO (number of exposures per offset). The instrument takes NEXPO exposures at a given offset position, then offset the telescope to a new position. In total, NOFF x NEXPO exposures are taken by the template. It is normally recommended to use NEXPO=1 and always do a small offset between subsequent exposures.

The use of the (S)KY exposure type allows the user to select less crowded regions on sky to take exposures which will be used for sky evaluation / sky subtraction. The typical exposure time of these SKY positions is shorter than the OBJECT ones, but will depend on the actual conditions of the observations. Typically, in dark time one gets ~0.75e⁻/min at 550nm from the sky while the RON is ~2.5e⁻ rms (i.e. variance 6.25) on average. The transition between read-out noise limited and sky-noise limited conditions occurs after about 10 min in dark time.

Similarly to other VLT instruments, telescope offsets are defined relative to the previous telescope position, therefore **the offsets are cumulative**, e.g. a sequence of [0, -2, 4, -2] will finish at the original position. The offsets are defined in units of arcseconds in the reference frame selected (DETECTOR or SKY). The convention is detailed below in Figure 20. If the first image is to be taken at the preset coordinates, the first set of offsets should be 0,0. If there are less offset values than the defined total number of exposures, the template will return at the beginning of the list of offsets and apply them again. However, **the number of offsets provided should be identical in x and y directions**.

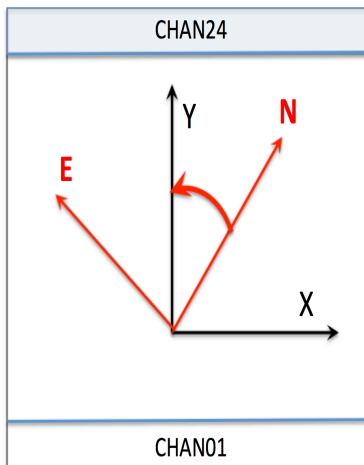
For example, if the number of exposures is 5 and the series of offsets (in "SKY" convention) is:

RA	0	-10	5
DEC	2	7	3

Then the offsets applied to the telescope will be:

ΔRA_{VLT}	0	-10	5	0	-10
ΔDEC_{VLT}	2	7	3	2	7

In addition, the user can provide a list of PA offsets to be sent to the instrument before starting the exposures at the new position. Like telescope offsets, PA offsets are cumulative. **When in "DETECTOR" framework, if both telescope offsets and PA offset are provided, the telescope offsets are sent with respect to the current PA of the instrument, before applying the PA offset.**



- If the user offsets are given in "SKY" convention, telescope offsets are sent in arcsecs, positive in the direction of East (RA) and North (DEC), respectively.
- If the user offsets are given in "DETECTOR" convention, telescope offsets are sent in arcsecs, positive in the X and Y directions, respectively, where the X and Y axes are defined relative to the 24 channels of MUSE.
- The **position angle** of a MUSE observation is measured positive East from North (red oriented angle). Positive position angle offsets are sent to the derotator in the same direction (see examples below).

Figure 22: Offset conventions for MUSE. We summarize here the main definitions

Example 1: Telescope offsets only, "SKY" convention

Total number of offsets: 5

Number of exposures per offset: 1

List of exposure types: O,S,O,O,S

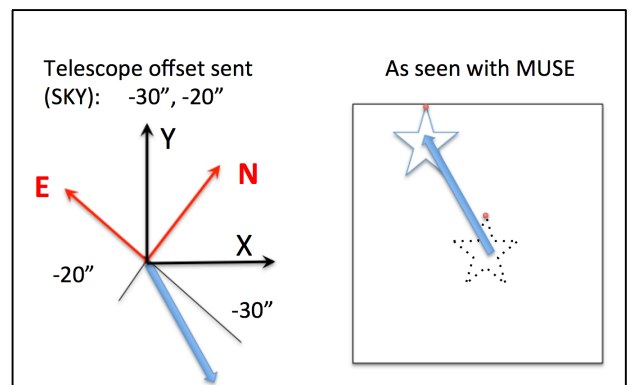
List of integration times: 1200,20,1200,1200,20

Offsets coordinate type: SKY

List of ΔRA offsets: 0,-30,30,-1,-29

List of ΔDEC offsets: 0,-20,20,3,-23

List of PA offsets: 0

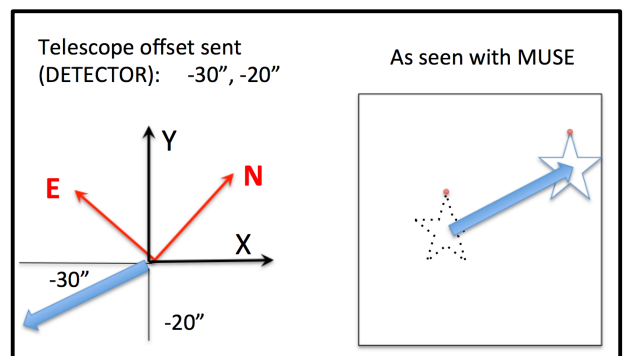


- ⇒ The telescope will (1) not move but make an 'object' exposure (1200s), (2) move and make a 'sky' exposure (20s), (3) move back to the origin and make an 'object' exposure (1200s), (4) move slightly and make an 'object' exposure (1200s), (5) move to the previous 'sky' position and make a 'sky' exposure (20s).

An illustration of the effect of the second offset is given in the figure.

Example 2: Telescope offsets only, "DETECTOR" convention

Total number of offsets: 7
 Number of exposures per offset: 1
 List of exposure types: S,O
 List of integration times: 20,1200
 Offsets coordinate type: DETECTOR
 List of X offsets: -30,30
 List of Y offsets: -20,20
 List of PA offsets: 0



- ⇒ The telescope will (1) move and make a 'sky' exposure (20s), (2) move back to the origin and make an 'object' exposure (1200s), (3) to (7) repeat (1) and (2) until 7 exposures have been taken: therefore the last exposure will be of 'sky' type, and the telescope will finish the template at the 'sky' position, shifted from the preset coordinates.
- ⇒ Note that the list of integration times could be '20,1200,20,1200', the result would be the same, as well as if the X list was '-30,30,-30,30,-30,30': each list is repeated as many times as required by the total number of exposures, and only the X and Y offsets list lengths are linked.

An illustration of the effect of the first offset is given in the top-right figure.

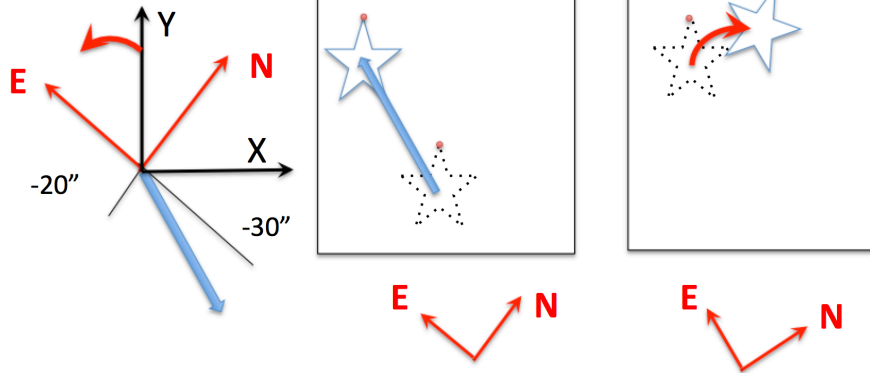
Example 3: Telescope offsets and PA offsets, "SKY" convention

An illustration of the effect of a (-30",-20") sky offset combined with a PA offset of 20 degrees is given in the figure:

Telescope offset sent (SKY): $-30''$, $-20''$

PA offset: $+20$ deg

As seen with MUSE



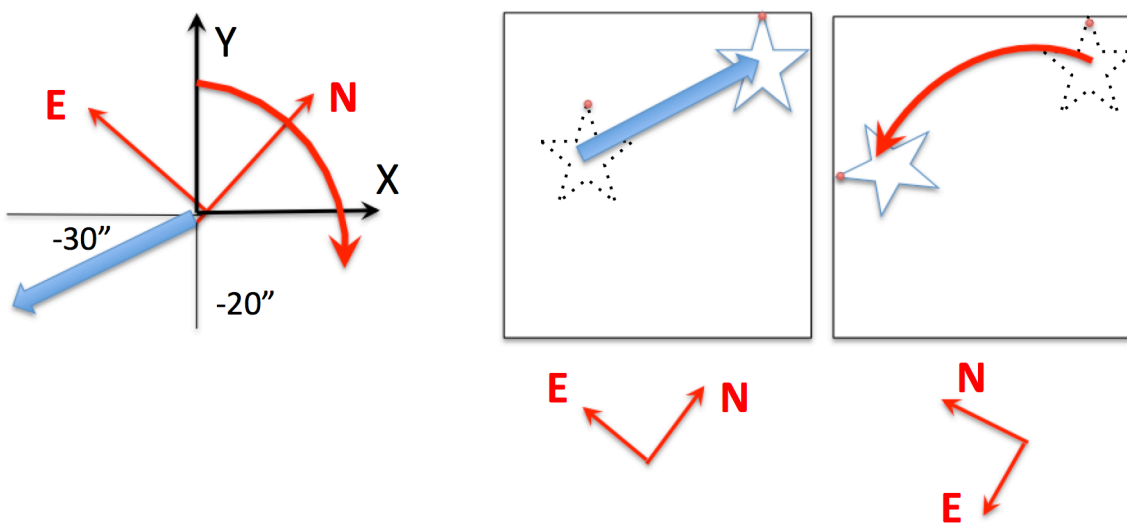
Example 4: Telescope offsets and PA offsets, “DETECTOR” convention

An illustration of the effect of a $(-30''$, $-20''$) detector offset combined with a PA offset of -100 degrees is given in the figure:

Telescope offset sent (DETECTOR): $-30''$, $-20''$

PA offset: -100 deg

As seen with MUSE





5.5 Attached calibrations

Calibrations taken regularly during operations (Section 6) provide daily flat-field and arc exposures, and illumination correction exposures are taken according to thermal variations during the night to account for repeatability (Section 6.1.3). If a MUSE observer believes more accuracy is needed it is possible to include arc and flat calibration in an observing OB as an attached calibration template, directly after the corresponding science template. Such attached calibrations are not recommended at this stage and are charged to the user program.

5.6 Instrument and Telescope Overheads

We provide here a summary of the telescope and instrument overheads (Table 10).

Table 10: Summary of overheads.

Acquisition and setup		
Telescope pointing, guide star acquisition (Preset)	360 s	
Interactive acquisition loop	18 s	
AO loops closure (in WFM-AO modes only)	180 s	
SGS loop closure	20 s	
Observations		
Detector setup	15 s	
Detector readout + FITS file merging	60 s	
Intra-exposure detector delay (for multiple exposures)	5 s	
Small telescope offset (< 2 arcmin)	15 s	
Large telescope offset (> 2 arcmin)	45 s	
SGS loop closure after offsets	15 s	
Derotator offset	5 s + 0.11 s / degree	
Attached calibration	Attached flat-field calibrations	240 s + 106 s / flat-field
	Attached wavelength calibration	180 s + 112 s / arc lamp exposure (1 per lamp)



Return to origin	0 s if no offsets 15 s if there was no large offset 45 s if there was at least one large offset
------------------	---

Execution time computations:

Example 1 : small telescope offsets, no PA offsets, no-AO mode

$$T_{total} = 360 \text{ s (preset)} + T_{acq} + 18 \text{ s (acquisition, 1 iteration)} + 20 \text{ s (SGS loop closure)} + N \times (15 \text{ s} + \text{UIT} + 60 \text{ s}) + (N-1) \times [5 \text{ s (intra-exposures delay)} + 15 \text{ s (small telescope offset)} + 10 \text{ s (SGS loop closure)}] + 15 \text{ s (return to origin)}$$

With T_{acq} the integration time of acquisition and UIT the integration time of each of the N exposures (assuming identical UITs).

Example 2: large telescope offsets and 90 degrees PA offsets between exposures in WFM-AO mode

$$T_{total} = 360 \text{ s (preset)} + T_{acq} + 18 \text{ s (acquisition, 1 iteration)} + 180 \text{ s (AO loops closure)} + 20 \text{ sec (SGS loop closure)} + N \times (15 \text{ s} + \text{UIT} + 60 \text{ s}) + (N-1) \times [5 \text{ s (intra-exposures delay)} + 45 \text{ s (large telescope offset)} + 5 \text{ s} + 0.11 \text{ s} \times 90 \text{ (rotation)} + 10 \text{ s (SGS loop closure)}] + 45 \text{ s (return to origin)}$$

With T_{acq} the integration time of acquisition and UIT the integration time of each of the N exposures (assuming identical UITs).

An alternative easy way to calculate the overhead is to create a MUSE OB by using the P2PP in tutorial mode (login: 52052, password: tutorial) and then run the time calculator software, which provides the total integration and execution time.

We request that during phase I service mode users divide their total shutter open time for each target into one hour OBs using p2pp and provide this info in the Time Justification section of the proposal.



6 Calibrating and Reducing MUSE data

6.1 MUSE calibration plan

We summarize below the main calibrations performed as part of the standard calibration plan for MUSE. These calibrations are performed on a regular basis. The definition of the calibration plan is still work in progress at this stage.

Calibration	Number of exposures (per mode)	Frequency	Phase	Purpose
Bias	11	Daily	Day	Master bias, bias characteristics
Dark	3	Monthly	Day	Master dark, dark current
Flat-field with continuum lamp	11	Daily	Day	Illumination correction, Tracing solution, Background light, Instrument throughput
Wavelength	5 per lamp: Ne, Xe, HgCd	Daily	Day	Wavelength solution Dispersion characteristics
Geometrical calibration: multi-Pinhole mask with arc lamps (HgCd and Neon Penray together)	80	Monthly	Day	Relative location of the slices
Flat-field with sky	>3	Weekly	Twilight	Illumination correction
Flat field illumination correction	1	Every 1-2h	Night	To account for temperature variations of illumination correction.
Attached Flat-field with continuum lamp	$N (b)$	<i>On request.</i>	Night	High-precision flat-fielding
Attached Wavelength	$N (b)$	<i>On request</i>	Night	High-precision wavelength solution
Spectrophotometric calibration	1	(c)	Night	Absolute flux calibration Telluric correction (d)
Astrometry	1	Monthly	Night	Astrometric model

Table 11: MUSE Calibration plan

- During Science Verification normal flat-field calibrations were also done between 1 to 3 times per night depending on temperature variations. Now we are obtaining approximately every 1-2 hours a very short flat **in nominal mode** for illumination correction in **both** modes.
- The number of exposures is defined by the user.
- During clear or photometric nights in which MUSE science OBs are executed
- Note that we do not observe a telluric star right after or before each exposure. If a telluric star is desired, then the user must provide it and the time will be charged to the program. OBX files of our standard stars can be found in the Tools section of the MUSE web pages.



6.1.1 Wavelength calibration

Wavelength calibration is performed on a daily basis. For each MUSE instrument mode used in science observation, 5 exposures are taken with each of the 3 available arc lamps (HgCd, Xe, Ne) illuminating the entire FOV. The location of these reference emission lines on the detector is used by the pipeline to derive an overall wavelength solution. Details on the emission line wavelengths are provided for each lamp as a reference in Table 14 to Table 16, Section 8.2.

MUSE observers can submit an “attached” wavelength calibration to be performed directly following their science observation (not recommended).

6.1.2 Flat-field calibration

Every day and for each MUSE instrument mode used in science observation, 11 exposures are taken with the continuum lamp illuminating the entire FOV. The data reduction software uses these exposures to estimate the tracing solution, as well as the illumination and throughput as a function of position and wavelength.

During Science Verification, in addition to the daily calibrations, flat-field calibration observations were performed on a nightly basis, at a frequency of 1 to 3 times per night depending on temperature variations. After analysing the 2nd Commissioning observations of MUSE we have determined that a full set of flats is not necessary for the appropriate correction of the science data, and that instead we can use illumination correction observations taken during the night. These observations account for any temperature dependence of the flat field. See below.

MUSE observers can submit an “attached” flat-field calibration to be performed with the continuum lamp directly following their science observation (not recommended).

6.1.3 Nightly illumination correction

Every hour the system asks the observer to obtain an illumination correction observation. This is a single flat field in Nominal mode which is used by the pipeline to correct for any temperature variation in the illumination pattern of the slices. The service mode or visitor mode users do not need to provide an OB for this calibration.

6.1.4 Twilight sky flat calibration

This calibration takes evening twilight exposures to correct for overall illumination on sky.

Exposures are taken according to the sky brightness:

- a reference exposure is taken, and the average ADU level is estimated.
- Depending on this level, we estimate the integration time for the next exposure required in order to maintain a constant (and high) ADU level.
- This sequence is continued until the conditions are no longer appropriate for twilight exposures or the maximum number of exposures to be taken is reached (whichever comes first)

6.1.5 Geometrical (spatial) calibration

Geometrical calibration is performed monthly. The instrument is set up in WFM with a multi-pinhole mask (WFM_SMP) covering the entire FOV (more details on this mask are given for reference in



Section 8.3). The mask is translated vertically by 0.034" between each exposure, and a total of 80 exposures are taken to fully cover all slices by the pinholes.

These exposures are analysed by the DRS to derive the relative location and orientation of each slice in each channel. Already processed geometry tables will be provided in the instrument package.

6.1.6 Spectro-photometric calibration

The spectro-photometric calibration is performed daily, whenever possible, using observations of a field containing a spectrophotometric standard star. Several high SNR exposures (~ 10 000 ADU at peak) of the star are used to derive the flux calibration curve. The stars used for this calibration are taken from the reference list of standard stars:

<https://www.eso.org/sci/observing/tools/standards/spectra.html>

Note that the peak flux level can vary depending on the seeing at the time of the exposure. The level mentioned above is for approximately 1" seeing. The user can expect variations by a factor of two above or below this level depending on conditions at the time of the observations.

6.1.7 Telluric Correction

To correct the spectrum from telluric absorptions there are two options. The first one is the use of the observations of one of the specphot stars as discussed in the previous section. This option is fully backed by the pipeline as long as the star used is in the list of MUSE specphot standards, and the template used to observe it is `MUSE_wfm_cal_telluric`. The second option is the use of the program Molecfit (Smette et al., (2015, A&A 576, A77) , Kausch et al., (2015, A&A 576, A78)) to fit the telluric absorptions directly in the target spectrum.

Note that the template `MUSE_wfm_cal_telluric` is not yet recognized by the pipeline through Reflex. It is recognized however through esorex as long as the star observed with this template is one of those supported by the pipeline. The External Verification Modules (EVMs) within P2PP automatically check that the target used with this template is a supported star. Additionally, from P98 onwards, esorex triggers a warning if it finds that the spectrophotometric or telluric standard templates were carried out with non-supported stars. A list of supported stars can be found in Table 12 and in the MUSE pipeline manual (<http://www.eso.org/sci/facilities/paranal/instruments/muse/doc.html>).



Star name	Ra (2000)	Dec (2000)	Comment
GD71	05:52:27.614	15:53:13.750	
HD49798	06:48:04.690	-44:18:58.400	
LTT3218	08:41:32.500	-32:56:34.000	
GD108	10:00:47.254	-07:33:31.010	
GD153	12:57:02.337	22:01:52.680	
EG274	16:23:33.750	-39:13:47.500	
GJ754.1A	19:20:34.920	-07:40:00.070	EG131, very good telluric
LTT7987	20:10:56.846	-30:13:06.640	
LDS749B	21:32:16.239	00:15:14.400	
Feige110	23:19:58.398	-05:09:56.160	

Table 12: List of spectrophotometric standard stars that are supported by the MUSE pipeline for telluric corrections.

6.2 MUSE data reduction

The output of an exposure with the instrument is a raw frame, which has the following multi-extension FITS format:

- **Primary extension (Extension 0, header only):** contains the keywords specific to the exposure and common to all channels, such as information about the observing program, telescope, overall instrument and weather conditions, etc. Note that some of the parameters monitored by the SGS system make it into keywords in the primary headers of the science images, the most important ones been OCS.SGS.FWHM.* and OCS.SGS.FLUX.*, that can be used to monitor the image quality and transparency during the exposure. But please note that the image quality monitoring keywords should be taken with caution because the SGS filter is very wide, and it is thus affected by atmospheric dispersion.
- **Extensions 1 to 24:** contains for each channel a short header (with information specific to the detector) and the image frame corresponding to this particular channel. The order of the extensions in the FITS file does not follow the order of the channel numbers so they should be addressed with their **extension name** CHAN01, CHAN02, CHAN03 CHAN22, CHAN23, CHAN24 corresponding to the channel number. The size of the image frame, in the absence of binning, is 4224 x 4240 (including the overscan regions, see Section 2.2.4.3).



- **Extension 25 to 27** (for science exposures) contain information from the SGS taken in parallel to the science exposures, when SGS is activated. The SGS will record images with the TCCD and produce stack median images every ~ 2 min. These median images can be averaged over the entire science exposure to give a deeper image of the region surrounding the MUSE FOV.
 - **Extension 25 (SGS_IMG)**: an image of size 1024x1024 contains the average of all the stacked median images taken during the science exposure.
 - **Extension 26 (SGS_CUBE)**: a cube of 1024x1024xN pixels, containing all N stacked median images taken during the science exposures.
 - **Extension 27 (SGS_DATA)**: a FITS table containing information from the SGS system in the form of (4+NSTARSx10)xN entries, for the N measurements done using NSTARS (NSTARS<10) stars detected in the SGS. For each measurement, the 4 first columns give general information about the time and the offsets sent to the telescope, while the last 10 x NSTARS entries give information on each star.
 - **Extension 28 (AG_DATA)**: a FITS table containing information about the guide star (GS) from the telescope Auto Guider (AG). It contains three columns giving the time of the measurement, and the fwhm in x and y, with a typical periodicity of 11 to 45 seconds. If there is no SGS star these data can be used to check the image quality during the exposure.

The MUSE Data Reduction Software (DRS) has been developed to fully reduce MUSE raw science observations using the associated calibrations. Data reduction is performed following a number of calibration recipes. The final output of the DRS is a FITS datacube (with RA, DEC and wavelength as the three axes), as well as a number of quality control (QC) parameters for each recipe. Full details on installing and using the MUSE DRS will be provided in the MUSE Pipeline Manual, which can be found at the webpage below:

<https://www.eso.org/sci/facilities/paranal/instruments/muse/doc.html>

Note that given the data volume and complexity of MUSE exposures, data reduction can be extremely resource intensive on computer architecture, especially on memory. It is not recommended that data be reduced on personal computer, rather a multi-core workstation with at the very least 32 GB RAM is recommended. However, for the end-cube production and combination of multiple datacubes a machine with at least 150 GB RAM is needed.

MUSE data are now processed by QC using the ESO calibration pipelines with the best available calibration data. The reduced datacubes (one per OB) can be downloaded directly from the Phase 3 query form in the ESO Archive.



7 Templates

7.1 MUSE acquisition templates

Full details on acquisition are provided in Section 5.3, including the parameters to define in P2PP. The main parameters of the acquisition are the instrument mode (WFM-NOAO-N or WFM-NOAO-E), position angle, exposure time for the acquisition, use of SGS, and definition of telescope guide star and/or blind offsets.

7.1.1 MUSE_wfm-noao_acq_movetopixel template signature file

MUSE_wfm-noao_acq_movetopixel.tsf		
KEYWORD	Range (Default)	Label in P2PP
<i>To be specified</i>		
DET.UIT1	0..120 (0)	Integration Time (seconds)
SEQ.SGS	T F (T)	Start slow-guiding?
TEL.TARG.OFFSETALPHA	-300..300 (0.0)	Alpha offset for the target (arcsec)
TEL.TARG.OFFSETDELTA	-300..300 (0.0)	Delta offset for the target (arcsec)
TEL.AG.GUIDESTAR	CATALOGUE/SETUPFILE/N ONE (CATALOGUE)	Get Guide Star from
TEL.GS1.ALPHA	0....240000 (000000.000)	RA of guide star (as HHMMSS.TTT)
TEL.GS1.DELTA	-900000.....900000(000000.000)	DEC of guide star (as +-DDMMSS.TTT)
INS.DROT.POSANG	0....360 (0)	Position Angle on Sky (deg)
INS.MODE	WFM-NOAO-E, WFM-NOAO-N	Instrument Mode

7.1.2 MUSE_wfm-ao_acq_movetopixelLGS template signature file

MUSE_wfm-ao_acq_movetopixelLGS.tsf		
KEYWORD	Range (Default)	Label in P2PP
<i>To be specified</i>		
DET.UIT1	0..120 (0)	Integration Time (seconds)
SEQ.SGS	T F (T)	Start slow-guiding?
TEL.TARG.OFFSETALPHA	-300..300 (0.0)	Alpha offset for the target (arcsec)
TEL.TARG.OFFSETDELTA	-300..300 (0.0)	Delta offset for the target (arcsec)
TEL.AG.GUIDESTAR	CATALOGUE/SETUPFILE/N	Get Guide Star from



	ONE (CATALOGUE)	
TEL.GS1.ALPHA	0....240000 (000000.000)	RA of guide star (as HHMMSS.TTT)
TEL.GS1.DELTA	-900000.....900000(000000.000)	DEC of guide star (as +-DDMMSS.TTT)
TEL.TTS1.ALPHA	00:00:00.000	RA of Tip-tilt star
TEL.TTS1.DELTA	00:00:00.000	DEC of Tip-tilt star
TEL.TTS1.RMAG	6..18.5	Mag. of Tip-tilt star
TEL.TTS2.ALPHA	00:00:00.000	RA of alternative Tip-tilt star
TEL.TTS2.DELTA	00:00:00.000	DEC of alternative Tip-tilt star
TEL.TTS2.RMAG	6..18.5	Mag. of alternative Tip-tilt star
INS.DROT.POSANG	0....360 (0)	Position Angle on Sky (deg)
INS.MODE	WFM-AO-E, WFM-AO-N	Instrument Mode

7.1.3 MUSE_wfm-noao_acq_preset template signature file

MUSE_wfm-noao_acq_preset.tsf		
KEYWORD	Range (Default)	Label in P2PP
<i>To be specified</i>		
SEQ.SGS	T F (T)	Start slow-guiding?
TEL.TARG.OFFSETALPHA	-300..300 (0.0)	Alpha offset for the target (arcsec)
TEL.TARG.OFFSETDELTA	-300..300 (0.0)	Delta offset for the target (arcsec)
TEL.AG.GUIDESTAR	CATALOGUE/SETUPFILE/NONE (CATALOGUE)	Get Guide Star from
TEL.GS1.ALPHA	0....240000 (000000.000)	RA of guide star (as HHMMSS.TTT)
TEL.GS1.DELTA	-900000.....900000(000000.000)	DEC of guide star (as +-DDMMSS.TTT)
INS.DROT.POSANG	0....360 (0)	Position Angle on Sky (deg)
INS.MODE	WFM-NOAO-E, WFM-NOAO-N	Instrument Mode

7.1.4 MUSE_wfm-noao_acq_presetRRM template signature file

This template should be used for rapid response mode, when observation of highly time critical targets is desired.



MUSE_wfm-noao_acq_presetRRM.tsf		
KEYWORD	Range (Default)	Label in P2PP
<i>To be specified</i>		
SEQ.SGS	T F (T)	Start slow-guiding?
TEL.TARG.OFFSETALPHA	-300..300 (0.0)	Alpha offset for the target (arcsec)
TEL.TARG.OFFSETDELTA	-300..300 (0.0)	Delta offset for the target (arcsec)
TEL.AG.GUIDESTAR	CATALOGUE/SETUPFILE/NONE (CATALOGUE)	Get Guide Star from
TEL.GS1.ALPHA	0....240000 (000000.000)	RA of guide star (as HHMMSS.TTT)
TEL.GS1.DELTA	-900000.....900000(000000.000)	DEC of guide star (as +-DDMMSS.TTT)
INS.DROT.POSANG	0....360 (0)	Position Angle on Sky (deg)
INS.MODE	WFM-NOAO-E, WFM-NOAO-N	Instrument Mode
<i>Hidden</i>		
SEQ.RRM.REGISTER	T, F (T)	(Register OB in RRM)
SEQ.RRM.VISITOR	T, F (T)	(Allow RRM activation in VM)



7.2 Observation Templates Tables

Full details on observing templates are provided in Section 5.4, including the main parameters to define in P2PP, in particular the definitions and conventions for offsets.

7.2.1 MUSE_wfm-noao_obs_genericoffset template signature file

MUSE_wfm-noao_obs_genericoffset.tsf		
KEYWORD	Range (Default)	Label in P2PP
<i>To be specified</i>		
SEQ.NEXPO	1..1000 (1)	Number of exposures per offset
SEQ.NOFF	1..1000 (NODEFAULT)	Total number of offsets
SEQ.OBSTYPE.LIST	O S (NODEFAULT)	Observation type list, O/S
SEQ.OFFSET.COORDS	SKY DETECTOR (SKY)	Offset coordinate type selection
SEQ.OFFSET.POSANG.LIST	-360..+360 (0)	List of relative offsets in position angle (deg)
SEQ.OFFSET1.LIST	-600..600 (NODEFAULT)	List of relative offsets in RA or X (arcsec)
SEQ.OFFSET2.LIST	-600..600 (NODEFAULT)	List of relative offsets in DEC or Y (arcsec)
SEQ.UIT.LIST	1 (NODEFAULT)	List of UITs



7.2.2 MUSE_wfm-ao_obs_genericoffsetLGS template signature file

MUSE_wfm-ao_obs_genericoffsetLGS.tsf		
KEYWORD	Range (Default)	Label in P2PP
<i>To be specified</i>		
SEQ.NEXPO	1..1000 (1)	Number of exposures per offset
SEQ.NOFF	1..1000 (NODEFAULT)	Total number of offsets
SEQ.OBSTYPE.LIST	O S (NODEFAULT)	Observation type list, O/S
SEQ.OFFSET.COORDS	SKY DETECTOR (SKY)	Offset coordinate type selection
SEQ.OFFSET.POSANG.LIST	-360..+360 (0)	List of relative offsets in position angle (deg)
SEQ.OFFSET1.LIST	-600..600 (NODEFAULT)	List of relative offsets in RA or X (arcsec)
SEQ.OFFSET2.LIST	-600..600 (NODEFAULT)	List of relative offsets in DEC or Y (arcsec)
SEQ.UIT.LIST	1 (NODEFAULT)	List of UITs

7.3 Calibration Templates Tables

7.3.1 Templates specifically written for night astronomers

These templates perform wavelength and internal flat calibration directly following a science exposures, at the same telescope and derotator position. These calibrations are useful when a very accurate wavelength or flat-field correction is necessary for the science observations, and they are charged to the User Program.

7.3.1.1 MUSE_wfm_cal_waveatt

This template is the equivalent of MUSE_wfm_cal_wave in case of attached calibration. The default values are those used during the daily calibrations.

MUSE_wfm_cal_waveatt.tsf		
KEYWORD	Range (Default)	Label in P2PP
<i>To be specified</i>		
SEQ.LAMP3.UIT	0..3600 (0.7)	Integration time on Neon penray lamp (s)
SEQ.LAMP4.UIT	0..3600 (19)	Integration time on Xenon penray lamp (s)



SEQ.LAMP5.UIT	0..3600 (1)	Integration time on HgCd High Power lamp (s)
SEQ.LAMP6.UIT	0..3600 (0)	Integration time on Neon High Power lamp (s)
SEQ.NEXPO	1..1000 (3)	Total number of exposures

7.3.1.2 MUSE_wfm_cal_specflatatt

This template is the equivalent of MUSE_wfm_cal_specflat in case of attached calibration. The default values are those used during the daily calibrations.

MUSE_wfm_cal_specflatatt.tsf		
KEYWORD	Range (Default)	Label in P2PP
<i>To be specified</i>		
DET.UIT1	0..3600 (0.4)	Integration Time (seconds)
SEQ.NEXPO	1..1000 (11)	Total number of exposures



7.3.2 Other calibration templates

7.3.2.1 MUSE_cal_bias template signature file

Parameters for bias exposures include: number of biases to be taken and the binning factor (always 1 for science exposure).

MUSE_cal_bias.tsf		
KEYWORD	Range (Default)	Label in P2PP
<i>To be specified</i>		
SEQ.NEXPO	1..1000 (11)	Total number of exposures

7.3.2.2 MUSE_cal_dark template signature file

This template is used to perform dark calibrations.

MUSE_cal_dark.tsf		
KEYWORD	Range (Default)	Label in P2PP
<i>To be specified</i>		
DET.UIT1	0..3600 (3600)	Integration time (seconds)
SEQ.NEXPO	1..1000 (3)	Total number of exposures

7.3.2.3 MUSE_wfm_cal_geometry template signature file

This template is used to perform the geometrical calibration, as described in Section 6.1

MUSE_wfm_cal_geometry		
KEYWORD	Range (Default)	Label in P2PP
<i>To be specified</i>		
SEQ.NEXPO	1..1000 (80)	Total number of exposures
SEQ.ONTIME.LIST	"(40 0 40 0)"	List of lamp on time (s) (Neon Penray, Xenon Penray, HgCd, Neon High Power)
SEQ.YSHIFT	0..40.767 (0.069)	Y offset applied on the mask (arcsecs)
INS.MODE	WFM-NOAO-E WFM-NOAO-N (NODEFAULT)	Instrument Mode



7.3.2.4 MUSE_wfm_cal_specflat template signature file

This template is used to perform the daily flat-field calibration, as described in Section 6.1

MUSE_wfm_cal_specflat.tsf		
KEYWORD	Range (Default)	Label in P2PP
<i>To be specified</i>		
DET.BINY	1 4 (1)	Binning factor along Y
DET.UIT1	0..3600 (0.5)	Integration time in seconds
SEQ.NEXPO	1..1000 (5)	Total number of exposures
INS.MODE	WFM-NOAO-E WFM-NOAO-N WFM-AO-E WFM-AO-N (NODEFAULT)	Instrument Mode

7.3.2.5 MUSE_wfm_cal_wave template signature file

This template is used to perform the daily wavelength calibration, as described in Section 6.1

MUSE_wfm_cal_wave.tsf		
KEYWORD	Range (Default)	Label in P2PP
<i>To be specified</i>		
SEQ.LAMP3.UIT	0..3600 (0.7)	Integration time on Neon penray lamp (s)
SEQ.LAMP4.UIT	0..3600 (19)	Integration time on Xenon penray lamp (s)
SEQ.LAMP5.UIT	0..3600 (1)	Integration time on HgCd High Power lamp (s)
SEQ.LAMP6.UIT	0..3600 (0)	Integration time on Neon High Power lamp (s)
SEQ.NEXPO	1..1000 (5)	Total number of exposures
INS.MODE	WFM-NOAO-N WFM-NOAO-E WFM-AO-E WFM-AO-N (NODEFAULT)	Instrument Mode



7.3.2.6 MUSE_wfm_cal_twilight template signature file

This template is used to perform the twilight flat calibration.

MUSE_wfm_cal_twilight.tsf		
KEYWORD	Range (Default)	Label in P2PP
<i>To be specified</i>		
SEQ.ADU.TARGET	1..60000 (50000)	Target number of counts
SEQ.UIT.START.DAWN	0.1..600 (30)	Start integration time at dawn time (s)
SEQ.UIT.START.DUSK	0.1..600 (1.0)	Start integration times at twilight time (s)
SEQ.NEXPO	1..1000 (8)	Maximum number of exposures
INS.MODE	WFM-NOAO-E WFM-NOAO-N WFM-AO-E WFM-AO-N (NODEFAULT)	Instrument Mode

7.3.2.7 MUSE_wfm_cal_specphot template signature file

This template is used to perform a spectrophotometric standard star calibration.

MUSE_wfm_cal_specphot.tsf		
KEYWORD	Range (Default)	Label in P2PP
<i>To be specified</i>		
DET.UIT1	0..3600 (120)	Integration Time (seconds)
SEQ.NEXPO	1..1000 (1)	Number of exposures per offset
SEQ.NOFF	1..1000 (1)	Total number of offsets
SEQ.OBSTYPE.LIST	O S (O)	Observation type list, O/S
SEQ.OFFSET.COORDS	SKY DETECTOR (DETECTOR)	Offset coordinate type selection
SEQ.OFFSET.POSANG.LIST	-360..360 (0)	List of relative offsets in Position Angle (deg)
SEQ.OFFSET1.LIST	-600..600 (-7)	List of relative offsets in RA or X
SEQ.OFFSET2.LIST	-600..600 (-1.25)	List of relative offsets in DEC or Y



7.3.2.8 MUSE_wfm_cal_telluric template signature file

This template is used to perform a telluric standard star calibration.

MUSE_wfm_cal_telluric.tsf		
KEYWORD	Range (Default)	Label in P2PP
<i>To be specified</i>		
DET.UIT1	0..3600 (NODEFAULT)	Integration Time (seconds)
SEQ.NEXPO	1..1000 (NODEFAULT)	Number of exposures per offset
SEQ.NOFF	1..1000 (NODEFAULT)	Total number of offsets
SEQ.NEXPO	1..1000 (1)	Total number of exposures
SEQ.OBSTYPE.LIST	O S (O)	Observation type list, O/S
SEQ.OFFSET.COORDS	SKY DETECTOR (SKY)	Offset coordinate type selection
SEQ.OFFSET.POSANG.LIST	-360..360 (0)	List of relative offsets in Position Angle (deg)
SEQ.OFFSET1.LIST	-600..600 (0)	List of relative offsets in RA or X (arcsec)
SEQ.OFFSET2.LIST	-600..600 (0)	List of relative offsets in DEC or Y (arcsec)

7.3.2.9 MUSE_wfm_cal_astrom template signature file

This template is used to perform the astrometric calibration, on a regular basis.

MUSE_wfm_cal_astrom.tsf		
KEYWORD	Range (Default)	Label in P2PP
<i>To be specified</i>		
SEQ.UIT.LIST	(300)	List of UITs
SEQ.NEXPO	1..1000 (1)	Number of exposures per offset
SEQ.NOFF	1..1000 (1)	Total number of offsets
SEQ.OBSTYPE.LIST	O S (O)	Observation type list, O/S
SEQ.OFFSET.COORDS	SKY DETECTOR (SKY)	Offset coordinate type selection
SEQ.OFFSET.POSANG.LIST	-360..360 (0)	List of relative offsets in Position Angle (deg)
SEQ.OFFSET1.LIST	-600..600 (0)	List of relative offsets in RA or X (arcsec)



MUSE User Manual

Doc. Number: ESO-261650

Doc. Version: 7.00

Released on:

Page: 63 of 72

SEQ.OFFSET2.LIST	-600..600 (0)	List of relative offsets in DEC or Y (arcsec)
------------------	---------------	---



8 Reference material

8.1 Detector cosmetics

We provide in Table 13 for reference the detectors showing 1 or several bad columns, with the corresponding region affected on the detector.

Table 13: List of defects identified for each detector (arranged by channel) by the MUSE pipeline as a DQ issue. Each detector is identified by its name (DET_ID) and associated IFU number. The last columns gives (when relevant) the number of bad columns (bc), bad pixels (bp), and the rectangular region showing defects marked as [x1:x2,y1:y2] in pixel positions on the raw data frames.

CHANNEL	IFU	DET_ID	DET_INDE X	DQ Cosmetics
1	24	psyche	6	None
2	1	victoria	6	None
3	10	flora	6	2055bp(1bc) [1828,2058:4112]
4	4	juno	6	None
5	15	vesta	5	None
6	2	hebe	5	None
7	12	circe	5	6025bp(3bcs) [2800:2802,2057:4068]
8	3	massalia	5	None
9	18	thalia	4	None
10	20	lutetia	4	4111bp(2bcs) [2156,2057:4112]
11	21	parthenope	4	None
12	11	hygiea	4	2034bp(1bc) [1567,23:2056]
13	17	harmonia	3	2056bp(1bc) [1101,1:2056]
14	19	irene	3	None
15	15	astraea	3	None
16	8	pallas	3	None
17	7	thetis	2	None
18	16	iris	2	None
19	9	kalliope	2	None
20	6	fortuna	2	None
21	13	proserpina	1	2054bp(1bc) [1411,1:2054]
22	5	eunomia	1	2051bp(1bc) [2673,6:2056]
23	23	metis	1	None
24	22	melpomene	1	None



8.2 Arc lamps list

We provide in Table 14, Table 15 and Table 16 the list of lines identified in the arc lamps used for wavelength calibration.

8.2.1 HgCd arc lamp

Table 14: list of wavelengths and relative fluxes for the HgCd arc lamp.

Wavelength (Angstroms)	Relative Flux
4339.2232	30
4347.4945	80
4358.335	5500
4412.9894	2
4662.352	25
4678.1493	1200
4799.9123	3800
4916.068	85
4960.1	3
4980.64	0.5
5025.6	3
5045.8	0.5
5085.8217	7150
5120.637	0.5
5154.6605	32
5290.74	0.5
5316.776	1
5354.034	10
5365.5	0.5
5460.75	35000
5549.634	1
5675.81	8
5769.61	7000
5790.67	6600
5803.782	8

5859.254	4
5871.975	0.5
5890.2	1
6072.64	6
6099.1421	4
6111.495	2
6123.27	5
6234.36	18
6325.1661	11
6330.0133	2
6438.4695	2800
6716.34	15
6778.1157	1
6888.564	0.5
6907.46	160
6965	6
7067	8
7081.901	40
7091.86	13
7177.8	0.5
7269.9	2
7345.6704	25
7367.3	0.5
7372.5	1
7383.2	18
7397	4
7504.1	6
7514.8	8
7552.1	0.5
7603	2
7635.2	30

7675.2	2
7724.2	12
7728.825	22
7821.2	1
7948.2	10
8005	30
8006.1	2
8014.8	8
8067	3
8070.7	2
8013.8	10
8115.4	42
8163.4	1
8195.6	2
8200.3089	4
8264.2	8
8408.3	14
8424.5	13
8521.4	3
8625	140
8652.7	1
8758.1	6
8763	1
8773.1	0.5
8783.7	0.5
8887.5	0.5
8988.9	1
9039.2	1
9067.2	0.5
9123.1	10
9138	2



9243.1	5
9253.9	1

9255	15
9499	35

8.2.2 Xe arc lamp

Table 15: list of wavelengths and relative fluxes for the Xe arc lamp

Wavelength (Angstroms)	Relative Flux
4500.978	9
4524.6805	7
4582.7472	3
4603.03	1
4624.2756	33
4671.2258	70
4690.97	2
4697.0208	11
4734.1518	20
4792.619	4
4807.019	24
4829.708	15
4843.2934	13
4916.507	16
4923.152	21
4972.71	1
5028.2794	4
5044.92	0.5
5261.95	1
5292.22	2
5337.89	2
5392.795	1
5394.738	1
5418.02	2
5439.923	1
5440.39	1
5532.78	6

5552.385	1
5566.615	2
5567.77	2
5570.91	3
5697	3
5716	2
5824	7
5875.018	6
5889.12	1
5894.988	6
5934	7
5974.152	0.5
5978.29	0.5
5998.115	0.5
6030	4
6111.8	5
6163.8	6
6178.303	3
6179.665	10
6182.42	14
6198.26	5
6200.892	3
6201.49	2
6224.168	0.5
6261.212	1
6265.302	1
6273.23	0.5
6286.011	2
6293	3
6318.062	19
6333.97	0.5
6344.98	0.5

6355.77	0.5
6419	1
6469.705	12
6472.841	6
6487.765	7
6498.717	5
6504.2	7
6521.508	1
6533.159	3
6543.36	1
6554.196	4
6595.561	11
6608.87	0.5
6632.464	6
6668.4	20
6679.8	2
6728.008	30
6767.12	1
6778	6
6827.315	25
6846.8	8
6860.19	1
6866.838	6
6872.107	18
6882.155	50
6910.82	1
6925.53	7
6935.8	4
6976.182	12
6982.05	2
6991.65	0.5
7019.02	4



MUSE User Manual

Doc. Number: ESO-261650

Doc. Version: 7.00

Released on:

Page: 67 of 72

7035.53	1
7048	5
7078.46	0.5
7119.598	110
7136.57	0.5
7200.79	1
7244.94	4
7257.94	10
7262.54	3
7266.49	7
7284.7	38
7316.272	27
7321.452	22
7336.48	15
7355.58	8
7386.003	29
7393.793	36
7400.41	8
7424.05	3
7441.94	4
7451	5
7473	15
7492.23	3
7501.13	3
7514.7	1
7559.79	9
7584.68	80
7600.77	2
7642.024	290
7664.3	12
7740.31	6
7783.66	5
7790	1
7802.651	30

7881.32	8
7887.393	96
7937.41	6
7967.342	125
8003.26	1
8029.67	13
8057.258	48
8061.339	45
8101.98	8
8109.46	1
8118.29	0.5
8171.02	6
8206.336	215
8231.6336	20000
8266.52	120
8280.1162	8500
8297.71	2
8324.58	3
8346.8217	795
8372	2
8392.37	2
8409.1894	1370
8437.55	1
8522.55	7
8530.1	9
8576.01	30
8624.24	17
8648.54	56
8692.2	24
8696.86	23
8709.7	11
8739.37	180
8758.2	34
8819.4106	37800

8851.44	3
8862.32	240
8885.71	3
8908.73	125
8930.83	170
8952.3	6800
8981.05	45
8987.57	90
9025.98	17
9032.18	23
9045.4466	8888
9096.13	25
9112.24	5
9131.59	4
9152.12	10
9162.652	10800
9167.52	70
9203.2	45
9211.38	27
9222.39	6
9245.18	2
9301.95	33
9306.64	36
9334.08	1
9374.76	250
9412.01	65
9441.46	5
9442.68	30
9445.34	100
9488	4
9497.07	27
9505.78	3
9513.377	450
9585.14	6



8.2.3 Ne arc lamp

Table 16: list of wavelengths and relative fluxes for the Ne arc lamps

Wavelength (Angstroms)	Relative Flux
4704.3949	0.5
4708.8594	0.5
5031.3484	0.5
5037.7512	5
5080.383	3
5154.4271	0.5
5188.6122	0.5
5193.1251	0.5
5193.224	0.5
5203.8962	0.5
5210.5672	0.5
5222.3517	0.5
5234.0271	0.5
5298.1891	0.5
5330.7775	18
5341.0938	15
5400.5616	38
5433.6513	0.5
5562.691	7
5656.6588	8
5662.5489	0.5
5689.8163	5
5719.185	4
5748.2985	16
5760.5885	0.5
5764.4188	90
5804.4496	20
5811.4066	0.5
5820.1558	50
5852.4878	3250

5872.8275	40
5881.895	2700
5901.409	40
5906.4294	18
5913.633	6
5918.9068	2
5919.029	2
5934.4522	3
5944.834	4400
5961.6228	3
5965.471	25
5975.122	1250
5987.9074	16
5991.6477	3
6000.9275	4
6029.9968	1500
6064.5359	5
6074.3376	3800
6096.163	4800
6118.0187	1
6128.4498	270
6143.0627	10000
6163.5937	3700
6174.802	12
6182.146	20
6189.0649	2
6205.7775	6
6217.2812	3500
6246.7294	5
6266.4952	7000
6293.7447	4
6304.7893	2600
6313.6855	6
6332.766	9600
6382.9914	11500

6402.248	21000
6421.7044	2
6444.7118	7
6506.5277	12000
6532.8824	5500
6598.9528	7100
6652.0925	48
6678.2766	12000
6717.043	9200
6738.032	1
6929.4672	12450
7024.05	1300
7032.4128	34000
7051.2922	47
7059.1079	205
7112.3075	1
7173.938	2650
7245.1665	17000
7304.8422	1
7438.8981	5200
7472.4383	80
7488.8712	1000
7535.7739	920
7544.0439	370
7833.0281	0.5
7839.052	5
7927.1172	7
7936.9957	20
7943.1805	120
8082.4576	210
8118.5495	50
8128.911	20
8136.4061	250
8248.6826	5
8259.3795	45



8266.0769	97
8300.3248	620
8365.7464	85
8377.507	2900
8418.4265	470
8463.3569	52
8484.4424	22
8495.3591	1650
8544.6952	30
8571.3535	35
8582.9031	19
8591.2583	550
8634.6472	630
8647.0412	64
8654.3828	1050
8680.794	215
8681.9216	215
8704.1122	45
8771.6575	100
8781.969	1000
8792.5056	5
8830.9067	6
8853.8669	450
8865.701	240
8919.5007	102
8988.5564	25
9148.672	130
9201.7588	95
9220.468	72
9226.691	17
9275.5191	8
9300.8532	70
9310.5833	8
9313.9731	25
9326.5072	55
9373.3079	15

9425.3797	40
9459.211	18
9486.6825	18
9534.164	45
9547.4052	20
9665.42	45

8.3 Description of the WFM_SMP mask

The geometrical calibration is performed by translating a multipinhole mask covering most of the WFM FOV of the instrument (Figure 22). It is composed of 12 vertical lines of 57 pinholes covering a rectangular region of 55.6 x 58.5 arcsecs on each side with a regular grid. By translating the mask vertically we are able to have pinholes entering and exiting each slice of the instrument during the geometrical calibration.

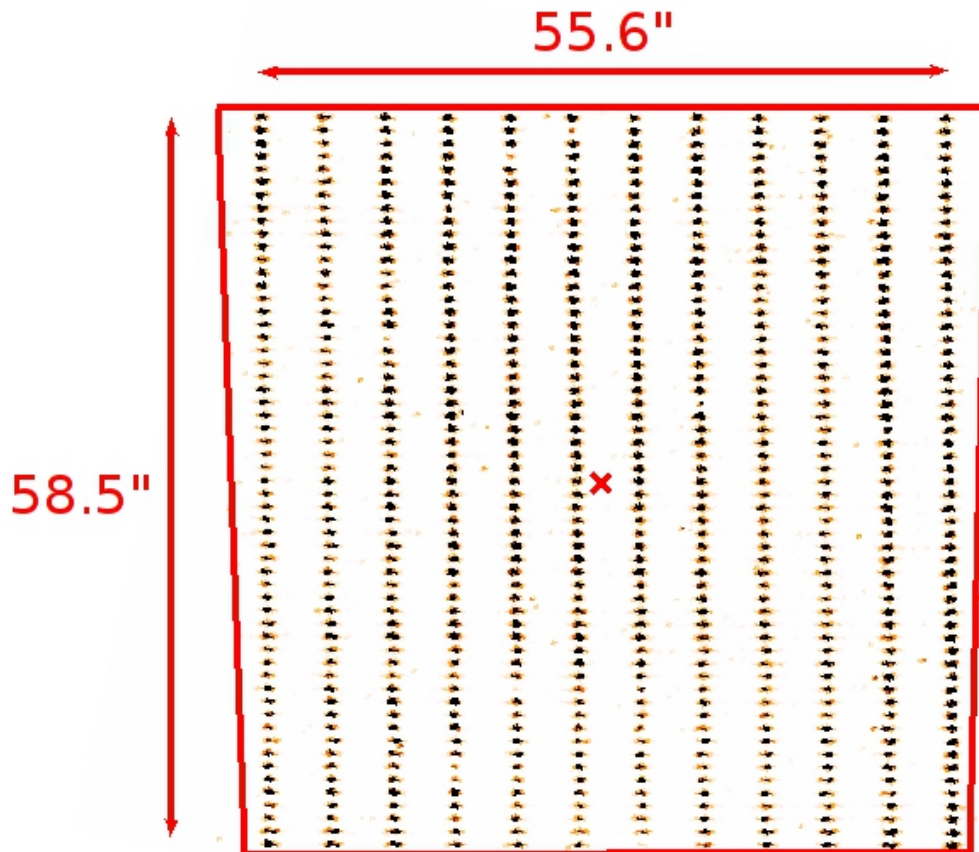


Figure 23: Arrangement of the WFM_SMP mask used for geometrical calibration, as viewed on a reconstructed image when illuminated with internal lamps. We overlay the trapezoidal shape of the FOV in red.



8.4 Log of instrument changes

Changes in software or hardware can have implications on the necessary calibration data set to reduce science data. For example, a change of detector invalidates all the previous bias, darks, flat fields, and geometry calibration files. For that reason we keep a table with all the changes in reverse chronological order. This table is kept in the ESO web at URL:

<http://www.eso.org/sci/facilities/paranal/instruments/muse/news.html>

8.5 ds9 template

We provide below the code used to create a ds9 template showing the trapezoidal FOV of MUSE in WFM mode, together with the SGS metrology field regions surrounding it.

One can simply copy/paste the code below in a MUSE_SGS_AO_TTS.tpl file and use it as a ds9 region template:

```
# Region file format: DS9 version 4.1
global color=green dashlist=8 3 width=1 font="helvetica 10 normal roman" select=1
highlite=1 dash=0 fixed=0 edit=1 move=1 delete=1 include=1 source=1
wcs0;fk5
# composite(359.9996,0.00034916642,3.983174e-09) || composite=1 color=red
circle(5.1688608e-05,0.00013316689,107.7") || # color=red
circle(5.1688608e-05,0.00013316689,51.75") || # color=red
polygon(0.0087104649,0.0083560229,0.00015906771,0.0084111669,359.99136,0.0085080189,35
9.99149,0.0020780231,359.9916,-0.0083669733,0.00071545399,-0.0084218338,0.008153512,-
0.008477959,0.008436852,-0.00031096806) ||
polygon(0.008768457,-0.008850979,359.99941,-0.008642834,359.99112,-
0.0087079895,359.99136,0.0087610189,1.2639545e-
05,0.0087301669,0.008876424,0.0085730173,0.0088858751,-0.00053898299) || #
color=magenta
polygon(0.0037316243,-0.012022859,0.0027164693,-0.012113846,359.9975,-
0.012069846,359.99619,-0.011962863,359.9961,-0.011647864,359.99522,-
0.011604879,359.99423,-0.0111519,359.99419,-0.010548901,359.99309,-
0.010455928,359.99246,-0.010024946,359.99172,-0.0094109694,359.99109,-
0.0088219905,359.99042,-0.008100015,359.98986,-0.0073900365,359.98944,-
0.0067840535,359.98908,-0.0061340687,359.98876,-0.0054420827,359.98841,-
0.0045710984,359.98811,-0.0037431118,359.98786,-0.0028251237,359.98768,-
0.0019231322,359.98758,-
0.00046213735,359.9876,0.0002008636,359.98767,0.0010258674,359.9878,0.0018848735,359.9
8797,0.0027278813,359.98829,0.0037878963,359.98859,0.00463091,359.98892,0.0054089246,3
59.98928,0.00617194,359.98977,0.00699796,359.99025,0.0077329787,359.99086,0.0084680012
,359.99157,0.0091280257,359.99234,0.0097690501,359.99325,0.010386076,359.99409,0.01088
2097,359.9951,0.011400118,359.99616,0.011741137,359.99725,0.012022151,359.99835,0.0121
99161,0.0020919472,0.012160159,0.0033024341,0.011940147,0.0041224391,0.011724135,0.004
9522032,0.011429121,0.0062407709,0.010824094,0.0080271721,0.0095930449,0.0088666732,0.
0088970177,0.0096378318,0.0080689903,0.01041874,0.0070549602,0.010994643,0.0060039365,
0.011551008,0.0047509123,0.011882864,0.0038118974,0.012175666,0.0027588838,0.012468457
,0.0015418699,0.012565979,-0.00040813479,0.012468289,-0.0019681301,0.012165615,-
0.0034091157,0.011911781,-0.004219104,0.011511518,-0.0052610859,0.011101507,-
0.0060670681,0.010603646,-0.0068940473,0.010047224,-0.0076180252,0.0090612974,-
0.008738989,0.0079875341,-0.0096849539,0.0068454527,-0.010549921,0.0063281113,-
0.010564908,0.0057131593,-0.010539894,0.0056643392,-0.011200893,0.0047175012,-
0.011681875,0.0037706732,-0.011702859) || # color=magenta
point(359.9996,0.00034916642) # point=x
```



MUSE User Manual

Doc. Number: ESO-261650

Doc. Version: 5.14

Released on:

Page: 72 of 72

Or download the MUSE.tpl file from the ESO webpages at

<https://www.eso.org/sci/facilities/paranal/instruments/muse/tools.html>

--- End of document ---